

# UCSF

## UC San Francisco Previously Published Works

### Title

Pathological changes of brain oscillations following ischemic stroke

### Permalink

<https://escholarship.org/uc/item/6jq696dm>

### Journal

Cerebrovascular and Brain Metabolism Reviews, 42(10)

### ISSN

1040-8827

### Authors

Sato, Yoshimichi  
Schmitt, Oliver  
Ip, Zachary  
[et al.](#)

### Publication Date

2022-10-01

### DOI

10.1177/0271678x221105677

Peer reviewed

# Pathological changes of brain oscillations following ischemic stroke

Yoshimichi Sato<sup>1,2,3</sup>, Oliver Schmitt<sup>4</sup>, Zachary Ip<sup>5,6</sup>,  
Gratianne Rabiller<sup>1,2</sup>, Shunsuke Omodaka<sup>1,2,3</sup>, Teiji Tominaga<sup>3</sup>,  
Azadeh Yazdan-Shahmorad<sup>5,6</sup> and Jialing Liu<sup>1,2</sup>

Journal of Cerebral Blood Flow & Metabolism  
2022, Vol. 42(10) 1753–1776  
© The Author(s) 2022  
Article reuse guidelines:  
sagepub.com/journals-permissions  
DOI: 10.1177/0271678X221105677  
journals.sagepub.com/home/jcbfm



## Abstract

Brain oscillations recorded in the extracellular space are among the most important aspects of neurophysiology data reflecting the activity and function of neurons in a population or a network. The signal strength and patterns of brain oscillations can be powerful biomarkers used for disease detection and prediction of the recovery of function. Electrophysiological signals can also serve as an index for many cutting-edge technologies aiming to interface between the nervous system and neuroprosthetic devices and to monitor the efficacy of boosting neural activity. In this review, we provided an overview of the basic knowledge regarding local field potential, electro- or magneto-encephalography signals, and their biological relevance, followed by a summary of the findings reported in various clinical and experimental stroke studies. We reviewed evidence of stroke-induced changes in hippocampal oscillations and disruption of communication between brain networks as potential mechanisms underlying post-stroke cognitive dysfunction. We also discussed the promise of brain stimulation in promoting post stroke functional recovery via restoring neural activity and enhancing brain plasticity.

## Keywords

LFP, modulation index, coherence, connectivity, sharp wave associated ripples

Received 18 October 2021; Revised 1 April 2022; Accepted 17 May 2022

## Introduction

Local field potential (LFP), commonly referred to as electroencephalography (EEG) in clinical neuroscience, records synaptic potential generated by groups of excitatory and inhibitory neurons as oscillating waves within the range of detection by the electrodes. Powered by evolving data science in decoding and pattern recognition, electrophysiology has provided crucial information in improving our understanding of normal brain function as well as altered function due to injury or diseases. The frequencies of these brain oscillations include the physiological range of <1 Hz to 250 Hz and can extend to a higher frequency range under pathological conditions such as seizure activity. Although the origin of brain oscillations can be widespread, it is generally believed that each wave serves a specific function among certain brain structures and networks. Brain oscillations exhibit complex patterns of interaction and regulation within brain structures, as well as between them, binding networks together

to achieve optimal functionality. Brain injuries and diseases often affect this tightly regulated coordination disproportionately, resulting in impaired brain function.

<sup>1</sup>Department of Neurological Surgery, UCSF, San Francisco, CA, USA

<sup>2</sup>Department of Neurological Surgery, SFVAMC, San Francisco, CA, USA

<sup>3</sup>Department of Neurosurgery, Tohoku University Graduate School of Medicine, Sendai, Japan

<sup>4</sup>Department of Anatomy, Medical School Hamburg, University of Applied Sciences and Medical University, Hamburg, Germany

<sup>5</sup>Department of Bioengineering, University of Washington, Seattle, WA, USA

<sup>6</sup>Department of Electrical and Computer Engineering, University of Washington, Seattle, WA, USA

## Corresponding author:

Jialing Liu, Department of Neurological Surgery (112C), University of California at San Francisco and Department of Veterans Affairs Medical Center, 1700 Owens Street, San Francisco, California 94158, USA.  
Email: jialing.liu@ucsf.edu

The generation and maintenance of a membrane potential involves the consumption of ATP; thus, cerebral blood flow (CBF) has a considerable effect on brain oscillations, with those in the higher frequency range being particularly prone to the immediate ramifications of energy deprivation. Assessing brain oscillation changes as biomarkers of disease progression, prognosis, and neurodegeneration in brain ischemia is especially valuable in brain health science. Increased signal power in low-frequency oscillations coincided with the reduction of high-frequency oscillations that were often observed among patients and laboratory animals following ischemic stroke (Examples of EEG traces and topographical maps are shown in Figure 1). Deafferentation of subcortical structures such as the thalamus following cortical lesion can also lead to propagation of low-frequency oscillations. Despite ample data from earlier studies in clinical strokes, EEGs no longer play a significant role in stroke detection or diagnosis due to the development of better-suited neuroimaging modalities. Magnetoencephalography (MEG),<sup>4,5</sup> which measures a brain's magnetic fields generated by electric currents, has a higher spatial resolution and deeper brain region accessibility has emerged as a more fitting electrophysiological tool in predicting stroke prognosis and functional recovery. In addition, an Electrocorticography (ECoG) with flexible microelectrode arrays records within the subdural space, can reach very high spatial resolution, and has a reduced noise level compared to EEG.<sup>6,7</sup> Unlike ECoG, MEG is non-invasive and often used to assess novel stroke rehabilitation strategies nowadays.

Contrary to the non-invasive nature of EEG, penetrating electrodes used in experimental studies enabled the investigation of deeper brain structures remote from the ischemic infarct. Among those structures is the hippocampus, which is crucial for memory function but is often spared from ischemic injury caused by Middle Cerebral Artery Occlusion (MCAO). Sharp wave associated ripples (SPW-R), a hippocampus-specific oscillation, is crucial in memory consolidation, relying on an intricate balance between excitatory and inhibitory networks and are vulnerable to the disruption caused by ischemia. In this review, we will start by providing an overview on the basics of LFP/EEG signals and their biological relevance, followed by a summary of findings reported in clinical and experimental strokes. We will discuss recent findings from experimental stroke studies highlighting how ischemic injury alters hippocampal brain oscillation and communication between brain networks. Lastly, we will discuss emerging technologies such as Brain Machine Interface (BMI) and brain stimulation and their potential in promoting functional recovery post stroke.

## Brain oscillations detected by extracellular recordings

### *Major brain oscillation and their biological function in humans and animals*

Most human extracellular electrophysiological data were initially derived from conventional EEG recordings of electrical activity in the superficial layers of the brain using non-invasive scalp macro-electrodes,<sup>8</sup> as opposed to the local field potential recordings from high impedance micro-electrodes placed in the deeper brain locations that have been used for experimental studies. Over time, non-invasive recording technology has evolved to high-density scalp EEGs,<sup>9</sup> high spatio-temporal resolution Magnetoencephalography (MEG), which is less influenced by the conductivity of the extracellular space, and high spatial resolution low noise ElectroCorticography's (ECoG) that records activity in the subdural space bypassing the skull and in-between tissue that distort the signal. Commonly described oscillations in mammalian brains range from 0.05 to 250 Hz in frequency, including the best-known waves  $\delta$  (1–4 Hz),  $\theta$  (4–8 Hz),  $\alpha$  (8–12 Hz),  $\beta$  (12–30 Hz) and  $\gamma$  (30–80 Hz). Examples of lesser-known oscillations include slow waves (0.3–1 Hz) that are slower than the  $\delta$  band, and high frequency oscillations (HFO) (80–250 Hz) that are faster than the  $\gamma$  band.<sup>10</sup> Among the fast oscillations, SPW-Rs (150–250 Hz) are a type of hippocampal oscillation crucial for memory consolidation,<sup>11</sup> while pathological High Frequency Oscillations (pHFOs) (200–600 Hz) are often recorded in the dentate gyrus during seizure generation and are distinct from physiological SPW-Rs.<sup>11</sup> Compared to the penetrating electrodes used in animal studies, the non-invasive human scalp EEG detection is limited in frequency range and prone to artifacts and noise.

A consensus regarding the anatomical regions where brain oscillations originate in mammalian brains has not been established due to inconsistent findings. Specific brain regions or networks may serve as the generator for some oscillatory frequencies, while others act as the resonators that respond to certain firing frequencies.<sup>12</sup> The two main oscillation generators of the non-REM sleep-associated slow-wave were reportedly located in the pyramidal neurons of the layers II/III, V, and VI of the neocortex, and in the Nucleus Reticularis Thalami (NRT) neurons of the thalamus. Corticothalamic, thalamocortical, and intracortical connections are all involved in synchronizing activities between the 2 generators.<sup>13</sup> Similarly, the  $\delta$  wave is generated by the thalamus and pyramidal cells located in layers II–VI of the cortex, whereas higher frequency oscillations like  $\alpha$  or  $\beta$  are believed

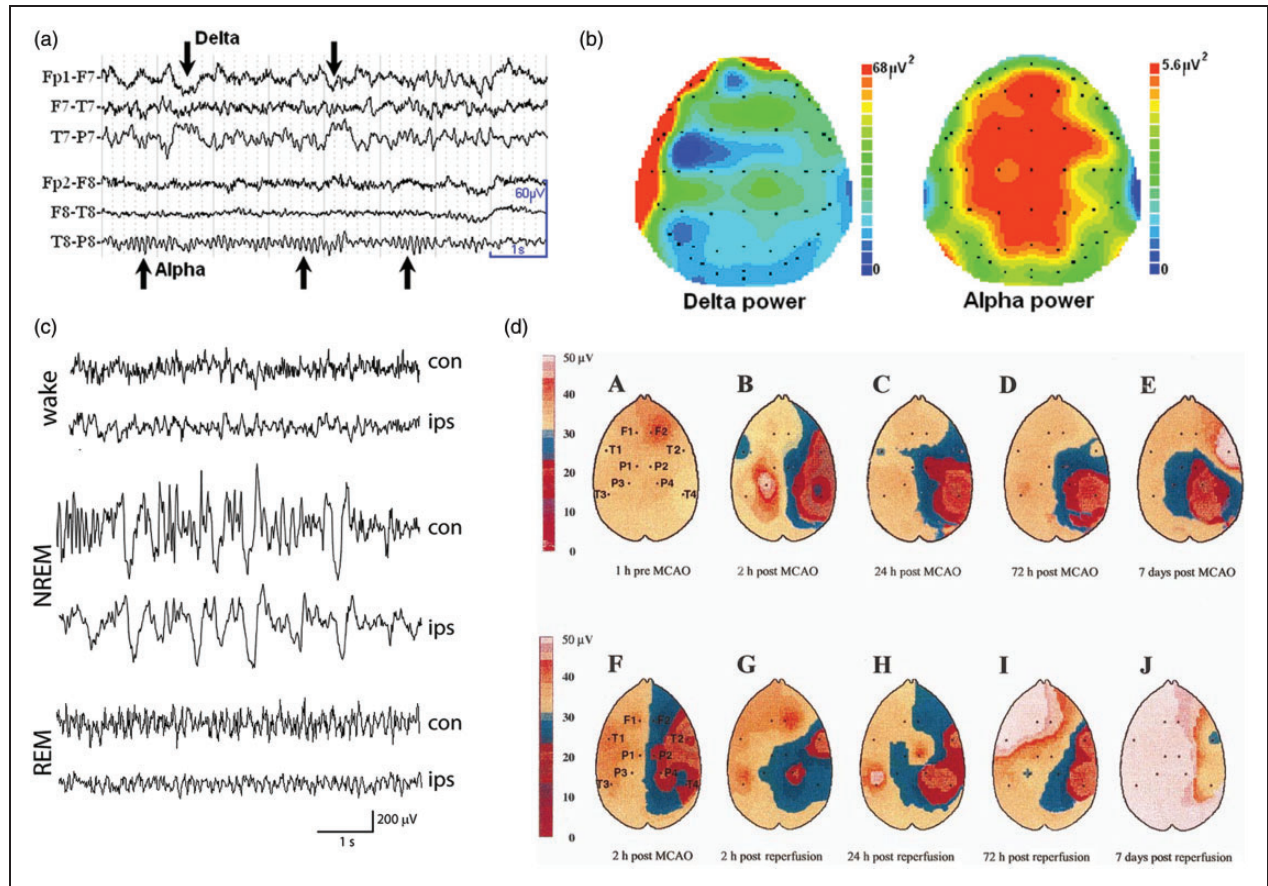


**Figure 1.** Examples of EEG traces and topographical maps from human and rat stroke. (a) The presence of delta wave in raw EEG traces recorded from a patient with left middle cerebral artery stroke (MCA) 7 hours after the onset of symptoms (NIHSS = 7). (b) Topographical maps showing the distribution of mean delta and alpha power across the scalp, with increased delta power in the frontal and temporal channels (adopted from figure 1, Finnigan and van Putten<sup>1</sup>) (c) Representative EEG traces of wake, rapid eye movement (REM) and nonrapid eye movement (NREM) sleep in ipsilesional (ips) and contralateral (con) hemisphere recorded 4 days after MCAO in a rat with pre-implanted epidural electrodes (adopted from figure 3, Leemburg S et al., 2018<sup>2</sup>) (d) Representative topographic EEG brain mappings of the amplitude of the global band selected at 5 time points from one rat with permanent MCA occlusion (a–e) and another with 2-hour temporary MCA occlusion (tMCAO) (f–j). (adopted from figure 9, Lu X et al., 2001<sup>3</sup>).

to be generated by the cells in layers IV and V of the cortex.<sup>14,15</sup> The hippocampus is known to resonate  $\theta$  oscillation that propagates through the septo-temporal axis via the volume conduction, since inactivation or lesion of the septum perturbs the hippocampal  $\theta$  oscillations.<sup>16</sup> However, discrepant studies have reported the hippocampal and thalamic origins of the  $\theta$  and  $\alpha$  waves, respectively. In contrast, the  $\gamma$  rhythm is widely spread among many brain structures including the cortex, midbrain and the hippocampus.<sup>17–19</sup> Low-frequency waves such as  $\theta$  and  $\delta$  propagate through the entire brain as directional waves, whereas high-frequency ones like  $\alpha$ ,  $\beta$ , and  $\gamma$  tend to stay localized to small structures and are driven by  $\theta$  and  $\delta$ .<sup>20,21</sup>

The functional role of each brain oscillation is complex, spanning from sensory motor to cognitive domains. Contributing to a dominant brain state, the

$\theta$  rhythm is involved in movement and cognitive activity during the awake state, as well as memory consolidation during non-REM sleep.<sup>22,23</sup> Conversely, the hippocampal non- $\theta$  state, also known as the slow-wave state (SWS), is associated with immobility or SWS sleep.<sup>24,25</sup> Manipulating the hippocampal  $\theta$  rhythm alters cognition, further suggesting a causal role of the hippocampal  $\theta$  in cognition.<sup>26</sup> Cortical  $\gamma$  oscillations, including low (30–60Hz) and high  $\gamma$  oscillations (60–150Hz), are known to play a role in sensory stimulation, declarative memory, attention selection, cognition, and assist in encoding and retrieval of memory traces in the hippocampal formation.<sup>27–29</sup> SPW-R, another novel and highly significant brain oscillation involved in cognition and memory, is discussed below. However, there are limitations in translating findings from animal studies to human

physiology with respect to age effect, the origin of brain oscillations and how they function across networks due to the species difference in brain structure and organization.

### *Sharp wave associated ripples (SPW-R)*

Experimental studies in recent decades have revealed a type of hippocampal oscillation with a frequency of 150-250 Hz that has not been described in human scalp EEG studies, known as the SPW-R. Detected in the CA1 pyramidal layer of the hippocampus, SPW-Rs are concurrent with the firing of sharp waves in the stratum radiatum, as the name implies. By now, ample experimental and human data have established that SPW-Rs play a crucial role in the formation and subsequent stabilization of enduring memories at the cortical level during system-level memory consolidation.<sup>11</sup> It has been reported the rate of SPW-Rs increase in the hippocampus of rats after learning a new task such as an odor-learning association or radial maze,<sup>30</sup> and their sequential activity is a replay of firing sequences of the same neurons activated during learning and exploration.<sup>31-36</sup> Conversely, the selective elimination of SPW-Rs via timed electrode stimulation during post-learning sleep resulted in the impairment of long-term memory.<sup>34-37</sup> Using intracranial recordings in human subjects engaging in episodic free recall of previously viewed pictures, a recent study found that content-selective increase in hippocampal SPW-R firing emerged 1-2 seconds before a recall event. SPW-R rate during encoding could also predict subsequent free recall accuracy, indicating that human memory reactivation during the free recall was coupled to hippocampal SPW-R events.<sup>38</sup>

SPW-Rs belong to a complex oscillatory network, the coupling of which coordinates specific information transfer among brain regions during memory consolidation. Combining neurophysiology recordings and fMRI techniques, a seminal study revealed the global effect of SPW-R in the brain. It was found that most of the cortical regions are activated during SPW-R, in contrast to the diencephalic, midbrain and brainstem regions are selectively inhibited.<sup>39</sup> This suggests that silencing the output of subcortical areas involved in sensory processing may minimize interference from regions like the thalamus and provide a privileged interaction state between hippocampus and cortex during memory consolidation. A later study confirmed the activity in the mediodorsal thalamic nucleus was suppressed during SPW-R firing in the awake state and around spindle-uncoupled SPW-R but was increased around spindle-coupled SPW-R during non-REM sleep.<sup>40</sup> This study confirmed that blocking thalamocortical relay of sensory information flow

facilitates memory consolidation in "off-line" learning during spindle-uncoupled SPW-R. This in turn promotes hippocampo-cortical communication because mPFC is more responsive to hippocampal input during spindle-uncoupled SPW-R. The interaction between hippocampal SPW-Rs and cortical slow waves appears to be bidirectional during NREM sleep.<sup>41</sup> In addition to the mediodorsal thalamic nucleus, other midline thalamic neurons such as the calretinin-positive neurons in the reuniens nucleus can also mediate hippocampus and mPFC interaction via SPW-R.<sup>42</sup>

Locally, both excitatory and inhibitory neurons are needed for proper SPW-R firing. Although the excitability of the pyramidal cells plays a key role in the generation of high frequency oscillatory events in the hippocampus, GABAergic activity is also crucially involved in maintaining SPW-R including GABA<sub>A</sub>R mediated signaling.<sup>43</sup> Direct evidence in support of the involvement of GABA in SPW-R regulation came from pharmacological studies in which focal pharmacological blockades of GABA<sub>A</sub> receptors abolished SPW-R,<sup>44</sup> while an antagonist of a GABA<sub>A</sub>R5 enhanced the power and duration of the SPW-R.<sup>45,46</sup> Specific targeting of GABA signaling via transgenic technology also affects ripples. By genetically reducing AMPA receptors in parvalbumin GABAergic interneurons in mutant mice, GABA-mediated tonic inhibition was altered and ripple oscillation was augmented.<sup>47</sup> Disturbance of physiological ripple oscillation has been reported after experimental stroke during acute and chronic phases.<sup>48,49</sup> Apart from ischemic stroke, changes in SPW-Rs are also observed in murine neurodegenerative disease models. For example, diminished ripple occurrence rates were found in aged mice with human Apolipoprotein E4 knocked in,<sup>50</sup> which led to the loss of hilar GABAergic interneurons,<sup>51</sup> while rTg4510 transgenic mice, a model of tauopathy and dementia, had reduced inhibitory control of the hippocampal network and smaller amplitude-SPW-R.<sup>52</sup> Therefore, a well-orchestrated action between excitation and inhibition is required for the normal physiological function of SPW-R since synchronous activation of excitatory pyramidal cells and certain classes of inhibitory GABAergic interneurons are necessary for SPW-R generation.<sup>43,53</sup>

It has recently been shown that prolonging SPW-R via optogenetic stimulation of the CA1 neurons improves memory performance.<sup>54</sup> SPW-R can also be enhanced pharmacologically, GABA inhibitor L655,708 reportedly enhances the power and duration of the SPW-R in rats,<sup>46</sup> and increases the SPW-R cluster in CA1,<sup>45</sup> although the efficacy of L655,708 in restoring SPW-R in disease or neurodegeneration has not been established.

### Complex interactions among brain waves

Most of the oscillations also show complex patterns of interaction with other waveforms or spike activities from other brain regions. Interaction between oscillations of different frequencies can occur via phase-amplitude coupling, resulting in synchronization of the amplitude envelope of faster rhythms within the phase of slower rhythms. The best-known example of cross-frequency phase coupling is the  $\theta$  modulation of  $\gamma$  amplitude that is known to play a critical role in cognition. During coupling,  $\theta$  oscillations provide a temporal reference for the exchange of information among different brain networks, whereas faster  $\gamma$ -frequency oscillations nested within  $\theta$  cycles underlie local information processing in the cortex.<sup>55,56</sup> Furthermore, the extent of cortical neurons modulated by  $\theta$  rhythm depends on neuronal location and subtype. A greater proportion of interneurons, for example, 32% in the parietal cortex and 46% in the prefrontal cortex, are modulated by  $\theta$  waves compared to that in pyramidal neurons (11% in the parietal cortex and 28% in the prefrontal cortex).<sup>57</sup> Breakdown of the phase-amplitude coupling disrupts communication between neural networks and causes disturbance of brain physiology or diseases. For example, the hippocampal  $\theta$ - $\gamma$  coupling is stronger during memory replay, while poor coupling predicts poor memory performance.<sup>58,59</sup> Similarly, reduced modulation of cortical  $\gamma$  amplitude during hippocampal  $\theta$  phase was reported in a mouse model for Alzheimer's Disease with cognitive deficit,<sup>60</sup> and in schizophrenic patients associated with working memory dysfunction.<sup>61</sup> A review of methods for EEG/LFP signal processing and data analysis can be found in supplemental material.

### EEG changes after cerebral ischemia

#### Effect of cerebral blood flow on EEG

The extracellular signal recorded in an EEG is the net summation of the electric current flow of charges in and out of the neurons, known as the current sink and source, respectively. Once activated, neurons release neurotransmitters into the synaptic cleft that either excite/depolarize or inhibit/hyperpolarize the adjacent postsynaptic neurons. The Excitatory Postsynaptic Potential (EPSP) depolarizes the postsynaptic neurons due to the release of excitatory neurotransmitters such as glutamate and acetylcholine, while Inhibitory Postsynaptic Potential (IPSP) hyperpolarizes neurons due to the release of inhibitory neurotransmitters such as  $\gamma$ -amino butyric acid (GABA) and glycine. Consequently, the summation of the IPSP and EPSP induces a graded potential in the

neuron so that when the membrane potential reaches the threshold, it induces an action potential that can be propagated between neurons. EEG detects field potential as IPSP or EPSP generated by neurons because those events are longer in duration than the action potential (up to 10 milliseconds vs. a few milliseconds). An EEG trace reflects the interaction of signals of a group of excitatory and inhibitory neurons within the detection range of the electrodes, in which the EEG waves oscillate with alternating rises and falls in amplitude.<sup>10</sup>

The maintenance of ionic gradients and membrane potential consumes energy, thus the reduction of cerebral blood flow (CBF) as a result of brain ischemia affects brain oscillations with differential sensitivity, in which the signal power of high frequency waves are first to be decreased at the early stage of hemodynamic failure.<sup>10</sup> Besides CBF reduction following ischemia, the concurrent increase of local glutamate release is also known to exacerbate the decrease of EEG power.<sup>62</sup> At the network level, attenuation of the excitatory drive onto the thalamus or enhanced subcortical inhibition from cortical lesions are known to cause thalamo-cortical dysrhythmia, often resulting in the propagation of low frequency oscillations (in the  $\delta$  and  $\theta$  range).<sup>63,64</sup> These stroke-induced thalamo-cortical pathological rhythms may underlie stroke-induced diaschisis such as neuropathic pain or hemispatial neglect.

#### Clinical Applications of EEG in acute ischemic stroke

Apart from being a non-invasive and a widely available device, the ability of an EEG to detect changes in brain electrical activity in real-time makes it a good candidate for monitoring the evolution and treatment of stroke. We discuss how the EEG signals are modified in stroke and how they can be used as biomarkers to predict prognosis after stroke.

Several reports indicate the utility of an EEG in acute ischemic stroke (Table 1). An EEG is highly sensitive to detect electrophysiological activities induced by ischemic stroke and could even detect changes in patients with no abnormal signs in the initial CT scan.<sup>67,76</sup> Due to advances in technology, it is possible to use an EEG anytime and anywhere through a more downsized and manageable portable version.<sup>77</sup> These options can be helpful in situations where time is of the essence, such as transportation of a patient via ambulance, or an initial assessment by paramedics. The prospect of being able to identify ischemic strokes earlier with the use of portable EEGs can expedite the necessary emergency treatments for ischemic stroke, such as intravenous thrombolysis and mechanical

**Table 1.** Summary of EEG characteristics in acute ischemic stroke.

Time of EEG recording relative to stroke	EEG biomarker	Main findings
<72 hr	Absolute spectral power	Stroke patients exhibited significant interhemispheric delta power asymmetry compared to non-stroke ( $p < 0.05$ ) <sup>65</sup>
<2 wk	Absolute spectral power	Lateralized theta and/or delta activity predicted ipsilateral cortical infarction (sensitivity 76%, specificity 82%) <sup>66</sup>
<24 hr	Topographic activity	Greater maximum delta power was observed in stroke vs non-stroke ( $p < 0.01$ ) <sup>67</sup>
<36 hr	Topographic activity	Increased delta and theta amplitude in stroke vs non-stroke patients <sup>68</sup>
<9 hr	Relative spectral power	Significantly greater mean delta power in stroke vs non-stroke patients ( $p < 0.01$ ) <sup>69</sup>
<24 hr	Tomography	Greater delta and theta and less alpha power in the territory of the stroke patients ( $p < 0.01$ ) <sup>70</sup>
<25 hr	RAWOD	A distinctive EEG pattern called RAWOD (Regional Attenuation WithOut Delta) can identify massive Ischemic stroke earlier than CT or MRI <sup>71</sup>
<72 hr	Relative spectral power, pdBSI	pdBSI distinguished stroke from control patients and TIA patients and correlated with clinical and radiological status ( $p < 0.001$ ) <sup>72</sup>
<24 hr	Relative spectral power	Greater delta, lower alpha, higher DAR, DTABR and Q Slowing in stroke vs non-stroke patients ( $p < 0.001$ ) <sup>73</sup>
<72 hr	Relative spectral power	Less theta power, more delta power, higher DAR and DTR in stroke vs non-stroke patients ( $p < 0.02$ ) <sup>74</sup>
<59 hr	Relative spectral power, BSI	Lower alpha power, greater delta power and higher DAR and DTABR in stroke vs non-stroke patients (all $p < 0.0001$ ) <sup>75</sup>
<72 hr	Relative spectral power	Analysis of variance with post hoc testing identified pronounced delta activity in stroke patients, while alpha and beta power were elevated in TI <sup>76</sup>
<72 hr	r-BSI	Higher r-BSI in stroke vs non-stroke patients ( $p = 0.002$ ) <sup>77</sup>
<24 hr	Relative spectral power	Higher DAR in stroke vs non-stroke patients (sensitivity 93%, specificity 94%) <sup>78</sup>

RAWOD: Regional Attenuation WithOut Delta; CT: computed tomography; MRI: magnetic resonance imaging; pdBSI: pairwise derived brain symmetry index; TIA: transit ischemic attack; BBSI: bilateral brain symmetry index; DAR: Delta:Alpha Ratio; DTABR: Delta:Theta:Alpha:Beta Ratio; DTR: Delta:Theta Ratio; BSI: brain symmetry index; r-BSI: revised brain symmetry index.

thrombectomy with the goal of improving the outcomes for said patients.

Similar to other experimental findings, greater  $\delta$  power and lesser  $\alpha$  or  $\beta$  activity was observed among stroke patients compared to healthy controls,<sup>71–73,92</sup> while increased or decreased  $\theta$  power have both been reported.<sup>74</sup> An asymmetric index such as the Brain Symmetry Index (BSI) or the global pair wise derived Brain Symmetry Index (pdBSI) is particularly instrumental in reflecting changes between both hemispheres over time. A significant asymmetry shown in BSI and pdBSI in brain waves was found in stroke patients compared to control.<sup>1,72,77</sup> Some studies indicated the size or location of the ischemic region was correlated to EEG changes.<sup>92</sup> Larger infarct volume was often associated with increased  $\delta$  and  $\theta$  power but with decreased  $\alpha$  and  $\beta$  power.<sup>69,93,94</sup> Another study showed a trend towards a reduction in faster waves in the contralateral hemisphere when infarct size was larger.<sup>93</sup>

As opposed to large infarct strokes, subtle focal  $\theta$  activity, asymmetries in the  $\alpha$  oscillation and mu rhythm were often detected in lacunar infarcts.<sup>95</sup> Abnormal EEG patterns were also reported and could result from the deafferentation of subcortical structures.<sup>92</sup> Interestingly, evidence suggests that EEG detection tends to show better sensitivity in the anterior circulation than the posterior circulation.<sup>66,67</sup> In addition, some recent studies suggest that an EEG can distinguish a transient ischemic attack (TIA) from an ischemic stroke. Evoked potentials and spectral power across all bands, with greater  $\delta$  power, less  $\alpha$  power and less  $\beta$  power were identified in TIA compared to ischemic stroke.<sup>76</sup>

**Continuous EEG monitoring during thrombolysis.** Reduction of  $\delta$  power before symptomatic recovery within 20 min after r-tPA administration was reported in human stroke patients,<sup>96,97</sup> consistent with finding in rodent

EEGs in which a significant increase in the amplitude and recovery of the BSI after early recombinant tissue Plasminogen Activator (r-tPA) administration (1–3 hr after photothrombotic stroke).<sup>98</sup> Another study showed a clear improvement of the BSI during the 6 hours after r-tPA administration.<sup>99</sup> These studies suggest that continuous EEG monitoring with real-time brain electrical activity information may help to identify successful recanalization by r-tPA. This identification could enable physicians to consider additional treatments such as intra-arterial thrombolysis or mechanical thrombectomy accordingly.

Moreover, continuous EEG monitoring may also detect secondary severe adverse events, such as massive hemorrhagic transformation, severe cerebral edema, stenosis, or re-occlusion in an early stage. However, a big limitation of the thrombolysis studies is the lack of real-time intra-arterial monitoring of the clot dissolving. Therefore, a study combining continuous EEG with intra-arterial therapy will clarify more detailed changes before and after recanalization.

#### *EEG as an electrophysiological biomarkers of stroke prognosis.*

Continuous EEG monitoring of ischemic stroke has become not only a tool to diagnose, but also a tool to predict the prognosis as an electrophysiological biomarker in the evaluation of functional outcome are frequently reported with the Modified Rankin Scale (mRS), Barthel Index/modified Barthel Index (BI/mBI), National Institutes of Health Stroke Scale (NIHSS) or mortality rate. Focal brain lesions may functionally impair remote regions, a phenomenon known as “diaschisis” in which the excitability and metabolism of the remote regions including the hemisphere contralateral to the stroke side are reduced.<sup>100,101</sup>

Greater  $\delta$  and  $\theta$  activity along with greater interhemispheric asymmetry, and lesser  $\alpha$  and  $\beta$  activity, appear to predict a bad prognosis in both acute and chronic phase ischemic stroke. One study reported the greater  $\delta$  and  $\theta$  power and lesser  $\beta$  and  $\gamma$  power within 24 hr from the onset was associated with poor mRS at discharge.<sup>102</sup> Another study found that lower BI at 21 days was associated with higher BSI at admission.<sup>103</sup> Furthermore, the NIHSS value was found to correlate with sBSI and pdBSI values,<sup>104,105</sup> while a greater contralateral  $\theta$  power was associated with increased mortality at discharge or six months post-stroke. Conversely, a lack of slow activity with minimal decrease in other background frequencies predicts a good outcome.<sup>106</sup>

EEG parameters evaluated during the pre-thrombolytic phase are indicative when predicting the prognosis of thrombolysis. One study reported the correlation between outcomes after treatment and the

pre-thrombolysis hyper-acute EEG parameters. Relative  $\delta$  power and  $\alpha$  power,  $\delta/\alpha$  ratio, and  $(\delta + \theta)/(\alpha + \beta)$  ratio significantly correlated with the seven-day and 12-month NIHSS, respectively. In an EEG study using the wireless and portable techniques, a good outcome as mRS  $\leq 2$  at 12 months was found strongly correlated to  $\delta/\alpha$  ratio,<sup>73</sup> suggesting these parameters in predicting short/long-term outcomes were not only feasible but might also contribute to the development of better treatment strategies. In conclusion, during ischemic stroke, the increase in lower frequencies and a decrease in faster frequencies are the main features. Persisting changes are associated with poor long-term functional outcome. The  $\delta$  wave change appears to be the most reliable index for reduced CBF and brain metabolism during focal ischemia.

#### *EEG/MEG to monitor post stroke functional recovery and efficacy of rehabilitation*

Magnetoencephalography (MEG) is a non-invasive measurement of the brain’s magnetic fields generated by electrical currents. The initial design of MEG by David Cohen in 1968 employed a copper induction coil for detection, which was plagued with noise.<sup>107</sup> Upon subsequent improvement, a superconducting quantum interference detector was able to successfully detect and measure the magnetic field. Direct measurement of brain function became possible with this technology that provides a very high temporal and spatial resolution image of neuronal activity. Since its early days being deployed as a device to evaluate the epileptic foci pre-surgically,<sup>108</sup> the clinical utility of MEG has expanded into many functional domains such as functional mapping of eloquent cortex. Mapping of the language cortex was found to be more accurate with MEG than with EEG due to the reduced noise level and lesser artifacts in the former.<sup>4,5,109</sup> As a result, MEG is now widely used for pre-operative brain mapping before brain tumor surgery because it is capable of detecting functional brain regions within the tumor.<sup>110</sup> The latest MEG has more than 250 sensors and provides a high spatial resolution and accessibility to deeper brain structures compared to the EEG. Recently, MEG has been introduced to solve the complex problems of recovery and brain reorganization after stroke. It is particularly instrumental in predicting the prognosis and in evaluating the efficacy of rehabilitation methods (Supplemental Table 1), which have become the new focus in the clinical use of MEG.

Unlike scalp EEG that detects electrical fields generated by extracellular currents, MEG primarily detects the magnetic fields induced by intracellular currents. As such, MEG possesses some major advantages over



EEG. First, the decay of magnetic fields as a function of distance is more pronounced than electrical fields, making MEG especially sensitive to superficial cortical activity. Consequently, MEG requires a smaller area of synchronized cortical activity to detect an epileptic spike relative to EEG. Second, MEG provides better spatial resolution of source localization than EEG, since magnetic fields are not distorted by tissue conductivity of the skull and CSF as in electrical fields. MEG is often combined with MRI to obtain an optimal structural perspective critical for brain mapping purposes (Figure 2). Although MEG is promising for diagnosing functional recovery and reorganization following a stroke, there are some limitations when applying it in actual clinical practice. MEG is much more expensive and time consuming compared to EEG. Additionally, it requires highly trained staff for data acquisition and analysis, limiting its accessibility. Despite its higher spatial resolution, the distance MEG is able to reach is inversely proportional to the magnetic flux density, making it difficult to assess deep brain structures. Under these conditions, the use of fMRI or PET would be good alternatives to assess these deeper structures.

Like an EEG, MEG detected a bilateral increase of the slow-wave activity and increase of interhemispheric asymmetry in the acute phase following a unilateral

ischemic stroke as a prediction of a worse functional outcome.<sup>112</sup> One study performed follow-up recordings of MEG in 16 patients with acute ischemic stroke of the MCA territory and found ~10-Hz oscillations enhancement in the temporoparietal lobes as a sign of recovery.<sup>113</sup> Another report evaluating 12 patients with ischemic or hemorrhagic stroke confirmed poor functional recovery among patients who showed no response to stimulation in the somatosensory evoked field.<sup>114</sup> This observation led to the hypothesis that intensive sensory peripheral stimulation may maximize the use of residual sensory function and thus contribute to the improvement of the sensory deficit. By calculating the size of hand representation in the primary somatosensory cortex, another study determined how upper extremity motor function was affected in 15 stroke patients and found that the enlargement of the hand representation predicted good recovery.<sup>115</sup> MEG can provide a novel way of indirectly assessing primary motor cortex projection and the extent of recovery of sensorimotor function by localizing cortical sources of response to median nerve stimulation in stroke patients,<sup>116</sup> which has proven to be of particular value among those who cannot perform motor tasks due to paralysis.

The application of various rehabilitation strategies in stroke subjects, such as Mirror Therapy (MT),

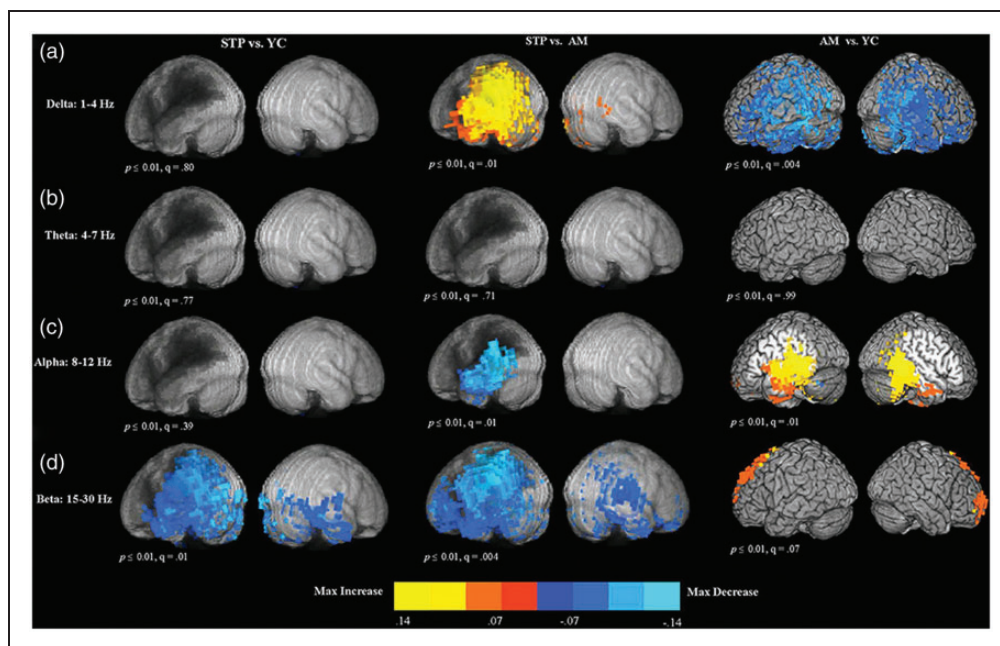


**Figure 2.** Age and stroke effect on brain oscillations detected by MEG. The maps represent the voxel-wise contrast resulting from a t-test comparing stroke and age effect (STP, stroke; YC, young controls; AM, age-matched). Resting-state data was collected for 5 min during MEG acquisition, followed by structural MRI scans. T-test comparison maps of relative delta power (a), theta power (b), alpha power (c) and beta power (d). Stroke increased the power of delta but decreased that of alpha and beta near lesion regions. To the contrary, age decreased delta, but increased alpha and beta power in specific brain regions (adopted from figure 4, Kielar A et al., 2016<sup>111</sup>).

Rhythmic Auditory Stimulation (RAS), Music Supported Therapy (MST) and speech therapy have been effectively evaluated by MEG in recent years. By creating a reflective illusion of a disabled limb with positive visual feedback of limb movement using a mirror, MT has shown to reduce the initial asymmetry in movement-related  $\beta$  desynchronization between hemispheres, according to a spinal cord injury study.<sup>117</sup> Another series of studies validated the benefit of using pulsed rhythmic or musical stimulation-supported motor rehabilitation to improve limb function in stroke patients with RAS or MST accompanied by showing enhanced connectivity between the auditory and motor network nodes for  $\beta$  and  $\gamma$  oscillations by MEG.<sup>118</sup> MEG was also introduced to evaluate the therapeutic effect of speech therapy in patients with aphasia to optimize the rehabilitation process, in which increased activation in the right hemisphere after speech therapy appeared to be related to language function recovery.<sup>119</sup>

#### *Using EEG/MEG in combination with brain machine interfaces (BMIs) for stroke rehabilitation*

The latest challenging application of MEG in stroke rehabilitation incorporates Brain–Machine Interface (BMI)<sup>120</sup> which circumvents the lack of feedback information commonly seen in stroke patients with low-mobility.<sup>121</sup> A recently developed BMI system allows stroke patients to control and manipulate a mechanical orthosis fixed to their paralyzed hand using mu-rhythm oscillations data detected by MEG in real time.<sup>122</sup> Compared to physiotherapy where patients can only move passively while simultaneously being told to imagine the active movement, BMI training is more proactive in improving a patient's motor abilities.<sup>123</sup> With BMI, MEG is transformed from a passive recording device into an active treatment and rehabilitation instrument in which the rapidly evolving technology is certainly anticipated. Similarly, studies have used EEG-based recordings to perform a virtual reach while simultaneously exciting a specific part of the peripheral nervous system according to Hebbian learning.<sup>124,125</sup> There is a large body of work regarding plasticity and the impact of BMI<sup>124–126</sup> and selective attention<sup>127,128</sup> that can lead to functional recovery from stroke. However, the functional recovery achieved with BMI technology among those patients remains modest due to several limitations: 1) Our insufficient knowledge of the neurophysiology correlates of recovery; 2) A substantial lack of understanding on strategies for targeted plasticity such as the timing between detected neural activity and peripheral stimulation; 3) Although BMI techniques focus on strengthening the connections between the brain and periphery

through the residual connections, emerging evidence suggests that targeted rewiring of the brain may lead to better a functional outcome<sup>124,129</sup> (see section 'Targeted stimulation-based therapies for stroke' for future potential directions).

#### **Local field potential changes after experimental stroke**

##### *Local field potential changes near ischemic infarct after experimental MCA occlusion*

Comparable to the changes observed in human stroke patients, the most consistent LFP/EEG characteristic during the acute and chronic phases of rodent focal ischemia was the increase of low-frequency and decrease of high-frequency oscillations (Table 2). Within a few minutes after MCAO, severe voltage suppression of LFP/EEG amplitude was observed in the ischemic hemisphere. Specifically following the temporary middle cerebral artery occlusion (tMCAO), the distribution of LFP/EEG changed from 25%–45% to 85% of  $\delta$  oscillations, from 40% to 7% of  $\theta$  oscillations, from 12%–15% to 5% of  $\alpha$  oscillations, and from 3–20% down to only 3% of  $\beta$  oscillations.<sup>3,130</sup> Following permanent MCAO (pMCAO), a reduction in LFP/EEG power across all frequency ranges was found in the ischemic ipsilateral cortex of rats acutely at 1–3 h and was associated with a decrease of 30% of CBF compared to baseline. Increased pdBSI was observed only in the acute phase of ischemia (from 15 min to one hour after occlusion) in young rats but up to 14 days in 12-month-old rats.<sup>91</sup>

Unlike neurons in the ischemic core where they can only depolarize in the presence of CBF at 20% below normal level, neurons in the penumbra can still repolarize following depolarization, but at the cost of perpetual depletion of valuable energy and the risk of core expansion.<sup>131</sup> During this critical period, sensory stimulation of the susceptible hot zone by tactile stimulation of the forelimb could trigger Peri-Infarct Depolarizations (PIDs) or spreading depression (SD), manifested as direct coupled potential shifts and suppressed electrocorticogram activity.<sup>132,133</sup> Therefore, post-stroke LFP/EEG monitoring can provide information into the evolution of the ischemic core and penumbra.<sup>104,134</sup> Detection of spreading depolarization requires direct current (DC) coupled recordings of local field potentials (LFPs),<sup>83,133</sup> although sometimes the spectral profile of the electrical events assessed by EEG and ECoG have been suggested to provide relevant information about SD, including its prediction.<sup>135,136</sup>

Table 2. Representative EEG/LFP studies in rat models of MCA stroke.

MCAO model	Time points of recording	State during recording	EEG/LFP biomarker	Main findings
Hours to 1 week f* tMCAO (120')	2 h–72 h	Anesthetized	Spectral power	EEG power suppressed at 2 h after MCAO and did not recovery by 24 h <sup>168</sup>
f tMCAO (120')	2 h–72 h	Anesthetized	Spectral power	EEG power reduced at 2 h after MCAO, some recovery by 24 h. Increase in power at 24 h <sup>169</sup>
f pMCAO	0.5 h–7 d	Anesthetized and freely moving (7 d)	Spectral power, spike-wave complexes	Severe EEG reduction near core at 2 h. Increase in delta power at 24 h ipsilaterally. Increased delta, beta and alpha by 7 d contralateral cortex <sup>109</sup>
f tMCAO (120')	occlusion, reperfusion – 3 d	Anesthetized and freely moving (1–3 d)	Spectral power	EEG amplitude decreased within minutes after MCAO ipsilaterally. EEG shifted towards slower frequencies 1–3 d ipsilaterally <sup>170</sup>
f tMCAO (50')	occlusion, reperfusion – 3 d	Anesthetized and freely moving (6 h–3 d)	Spectral power	Severe EEG depression and slowing as early as 1 min after MCAO ipsilaterally. Increase in in delta power <sup>171</sup>
f tMCAO (120'), pMCAO	2 h–72 h	Freely moving	DC, EEG amplitude	Peri-infarct depolarizations (PID) occurred during occlusion and stopped 2 hr after reperfusion. A second phase of PID re-emerged 10–18 hr after reperfusion. EEG depression occurred current with DC shift. <sup>116</sup>
f tMCAO (120')	2 h–72 h	Freely moving	Spectral power	1–3 Hz rhythmic spiking periodic lateralized epileptiform discharges detected within 1 h of MCAO over penumbra regions without convulsion behavior in 81% rats; intermittent rhythmic delta activity recurred in the contralateral hemisphere with frontoparietal dominance <sup>119</sup>
f tMCAO (60')	1 h–72 h	Freely moving	Spectral power	Na channel blocker reduced diffuse polymorphic delta activity/power and infarct size <sup>121</sup>
f tMCAO (90')	3 h–7 d	Freely moving	Spectral power	>50% reduction of EEG amplitude during MCAO and slight recovery after reperfusion. Persistent reduction of alpha power at 12–72 h. Increased delta power 24–48 h <sup>121</sup>
dMCAO (60')	occlusion, reperfusion- 30'	Anesthetized	Spectral power, T/D, SPW-R, HFD, MI	Altered brain state and reduced T/D ratio after dMCAO. Increased SPW-R firing in CA1 and reduced theta-gamma phase-amplitude coupling during reperfusion between hippocampus and cortex <sup>45</sup>
Up to 1 month pMCAO	D1–28	Freely moving	Spectral power	Slowing of EEG. Increase in delta power and decrease in alpha power d1–28 <sup>120</sup>
ET-1 (150 pmole)	15'–14 d	Freely moving	Spectral power, PSD	Immediate suppression of EEG power: Slow waves appeared 1–3 d. EEG changes are location specific <sup>172</sup>
dMCAO (60')	2 w–1 M	Anesthetized	Spectral power, T/D, SPW-R, CSD, MI	Theta-gamma phase-amplitude coupling was reduced while SPW-R power was increased at 2 w and 1 M after dMCAO. Environmental enrichment normalized stroke induced increase in SPW-R power <sup>46</sup>

(continued)

Table 2. Continued.

MCAO model	Time points of recording	State during recording	EEG/LFP biomarker	Main findings
> 1 month f tMCAO (120')	10 w, 3, 7, 12 M	Freely moving	Video EEG	No spontaneously seizures were detected up to 1 year after MCAO <sup>173</sup>
ET-I (120 pmole) tMACO	2 h, 2, 4, 6, 12 M Up to 6 M	Freely moving Freely moving	Video EEG Video EEG, spectral power	Only 1 out of 35 rats had seizures <sup>174</sup> EEG power in 7–15 Hz decreased. No seizure observed <sup>175</sup> EEG suppressed in ipsilateral side but increased in contralateral side 15' after stroke. pdBSI asymmetry increased up to 1 h in young compared to 14 d in middle-aged rats <sup>111</sup>
ET-I (150 pmole)	15', 1, 4h, 1, 3, 7, 14d, 8 M	Freely moving	Spectral power; PSD, pdBSI	

f<sup>o</sup>: filament model of MCAO; tMCAO: temporary MCAO; pMCAO: permanent MCAO; DC: direct current; T/D: theta/delta; SPW-R: sharp wave associated ripples; HFD: high frequency discharges; MI: modulation index; PSD: power spectral density; CSD: current source density; pdBSI: power density brain symmetry index.

Because the LFP/EEG amplitude depends on CBF, the recovery of LFP/EEG anomaly is often reported after ischemic reperfusion, but to various extents and speeds. For example, an increase of  $\delta$  amplitude was observed in the ipsilateral hemisphere as early as one minute following intraluminal suture occlusion of the proximal portion of the MCA and lasted until the chronic phase, seven days or beyond;<sup>91,130</sup> or even in the contralateral cortex one to seven days after tMCAO.<sup>3,84,91</sup> However, the recovery of  $\alpha$  or  $\beta$  amplitudes may take longer. One report showed that  $\alpha$  amplitude decreased from day one to day 28 after pMCAO, another found a 35% reduction in the amplitude of  $\alpha$  and  $\beta$  oscillations in the ipsilateral hemisphere three to seven days after tMCAO.<sup>86</sup> However, some studies reported an increase of  $\beta$  oscillation activity by seven days in the contralateral cortex after stroke in tMCAO rat models.<sup>3</sup>

Similar to human stroke findings, some evidence implicates a correlation between the infarct volume and LFP/EEG changes. Acute  $\delta$  oscillations increase,  $\delta$  change index, pdBSI, relative  $\alpha$  percentage, relative  $\alpha$ - $\beta$  percentage, relative  $\delta$ - $\theta$  percentage,  $\delta/\alpha$  ratio, or  $\delta$ - $\theta/\alpha$ - $\beta$  ratio were also reported to correlate with a larger infarct volume.<sup>85</sup> Additionally, commonly reported abnormal LFP/EEG patterns in experimental strokes included polymorphic slow-wave  $\delta$  activity; intermittent rhythmic  $\delta$  activity consisting of readily identifiable brief (<10 s) rhythmic large-amplitude bursts in the 4–7 Hz range; non-convulsive seizures, electro graphically defined as rhythmic discharges with spike components of 1–4 Hz frequency; occasional rhythmic spike-and-waves and polyspike discharges, not accompanied by motor convulsions; periodic lateralized epileptic discharge, consisting of interictal spikes; and sharp or slow-wave recurring with a variable period of 1–8 s.<sup>84,85</sup> These changes are separate from the generalized or regional slow-wave activity and show a focal attenuation of a specific rhythm, usually the faster activity frequencies, and general attenuation or suppression of one or more brain oscillations.

### Local field potential changes in brain regions remote from MCA infarct

Recent advances in functional connectivity suggest shared neuronal activation patterns define brain networks linking anatomically separate brain regions.<sup>137,138</sup> The hippocampus is involved in memory function, yet direct ischemic lesions in the hippocampus are rarely observed in MCA stroke,<sup>48</sup> raising the question of how function is affected in regions remote from the stroke epicenter via stroke-induced change of brain connectivity and reorganization.<sup>139–141</sup> By means of a meso-scale connectome analysis using

the *neuroVIISAS* platform,<sup>142</sup> we previously found that all 6 damaged cortical regions caused by distal occlusion of the MCA (dMCAO) including the parietal cortex and somatosensory cortex, had a relatively high connectivity with brain regions involved in processing spatial information,<sup>143</sup> including reciprocal connections with the perirhinal cortex, lateral entorhinal cortex, postrhinal cortex, and non-reciprocal connections with the CA1 (Figure 3). The adjacency matrix clearly shows complete output connectivity of the lesioned regions with the ipsilateral entorhinal cortex. Thus, each of the lesioned regions is connected to the main input interface of the spatial learning system,

suggesting that dMCAO leads to deafferentation of the hippocampal circuitry.

**During acute stroke.** By recording local field potentials under urethane anesthesia via a linear electrode array spanning the dorsohippocampus to deep cortical layers above, we found that dMCAO acutely altered the brain state in the hippocampus with reduced high- $\theta$  state and increased low- $\theta$  state, rendering the LFP with a decreased T/D ratio as compared to the pre stroke recording.<sup>48</sup> This change is similar to the finding in human EEGs near ischemic infarct soon after stroke onset, suggesting that dMCAO affects neural activity

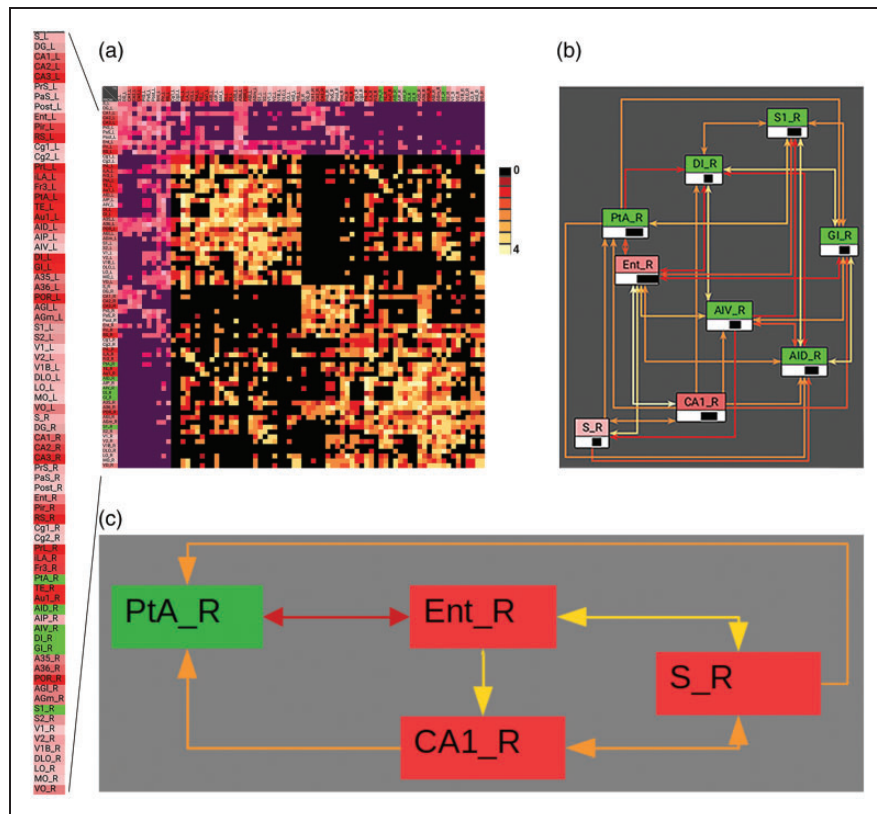


**Figure 3.** The lesioned cortical regions in the dMCAO stroke model are highly connected to ipsilateral limbic regions. Distal MCAO results in unilateral destruction of 6 cortical regions SI, GI, DI, PtA, AIV, AID (light green) and their neuronal connectivity.

(a) Overview of weighted and directional neuronal connections of neocortical and allocortical (magenta) regions. \_L: left hemispheric regions, \_R: right hemispheric regions. Significantly denser intrahemispheric connections between the lesioned regions and other brain regions compared to interhemispheric connections; Connection weights (0–4) were shown in color (black to yellow). The dense reciprocal and overlapping connectivity is evident between the lesioned regions and the limbic regions. The connectivity of lesioned right hemispheric regions was highlighted with the main input region (entorhinal cortex), output region (subiculum), and CA1 region of the hippocampal formation for ipsilesional hemisphere (b) and hippocampal-parietal cortex interconnectivity (c). Abbreviations: S: subiculum; DG: dentate gyrus; CA1/CA2/CA3: fields of hippocampus; Prs: presubiculum; PaS: parasubiculum; PostS: Postsubiculum; Ent: entorhinal cortex; Pir: piriform cortex; RS: retrosplenial regions; Cg1: cingulate cortex area 1; Cg2: cingulate cortex area 2; PrL: prelimbic cortex; iLA: Infralimbic area; Fr3: Frontal cortex area 3; PtA: parietal association cortex; TE: temporal cortex; Aul: primary auditory cortex; AID: agranular insular cortex dorsal part; AIP: agranular insular cortex posterior part; AIV: agranular insular cortex ventral part; DI: dysgranular insular cortex; GI: granular insular cortex; A35: perirhinal cortex A36: entorhinal cortex; POR: postrhinal cortex; AGI: lateral agranular prefrontal cortex AGm: medial agranular prefrontal cortex; S1: primary somatosensory cortex; S2: secondary somatosensory cortex; VI: primary visual cortex; V2: secondary visual cortex; VIB: primary visual cortex binocular area; DLO: dorsolateral orbital cortex; LO: lateral orbital cortex; MO: medial orbital cortex; VO: ventral orbital cortex.

in remote brain regions. During MCA occlusion, there was a temporary reduction of  $\theta$  and  $\gamma$  power bilaterally in the hippocampus, followed by a gradual recovery towards baseline level. The disturbance of signal power in  $\delta$ ,  $\theta$  and  $\gamma$  persisted after ischemic reperfusion.<sup>48</sup> There was also a significant increase in SPW-R s firing during ischemic reperfusion following MCA occlusion in the CA1 as accompanied by the sharp waves in the stratum radiatum compared to a few ripple events during baseline recording. In addition to SPW-R s, the occurrence of High-Frequency Discharges (HFD) in the range of 250–450 Hz was also increased during ischemic reperfusion following dMCAO (Figure 4), resulting in the increased proportion of HFDs in the pathological range compared to the physiological range of ripples.<sup>48</sup> The perturbation of either SPW-Rs or HFDs after stroke could be attributed to altered excitatory and inhibitory drives. For example, GABA<sub>a</sub>R and GABA<sub>b</sub>R are downregulated after hippocampal ischemia in guinea pigs<sup>144</sup> and focal ischemia in mice.<sup>145</sup>

Unlike the dMCAO model that produced an ischemic lesion mainly in the somatosensory cortex, unilateral hippocampal photothrombotic stroke caused an

extensive hippocampal infarction and reduced ipsilateral  $\gamma$  activity and elicited a direct current voltage shift. However, some HFDs in the range of 250–450 Hz recorded in the hippocampal photothrombotic model reminiscent of epileptiform discharges were also detected during the acute stage of our dMCAO model. This suggests that brain regions remote to the ischemic core could also suffer from similar electrophysiological perturbations.

Both cortical low (30–60 Hz) and high  $\gamma$  (60–120 Hz) bands engaged in dynamic and differential phase-amplitude modulation during acute stroke as demonstrated by the changes of the Modulation Index (MI). Increased MI between cortical high  $\gamma$  bands and hippocampal  $\theta$  (4–7 Hz) ( $MI_{HiG-\theta}$ ) or low frequency oscillations (0–4 Hz) ( $MI_{HiG-Lowfreq}$ ) was observed during MCA occlusion and the reperfusion period in the ipsilateral CA1 layer during high theta duration (HTD) but not low theta duration (LTD) phase. On the other hand, increased coupling of cortical low  $\gamma$  and hippocampal low frequency oscillations ( $MI_{LoG-Lowfreq}$ ) were found during MCA occlusion in bilateral CA1. Furthermore, the phase of the  $\delta$  wave along with cortical high  $\gamma$  coupled during MCA occlusion

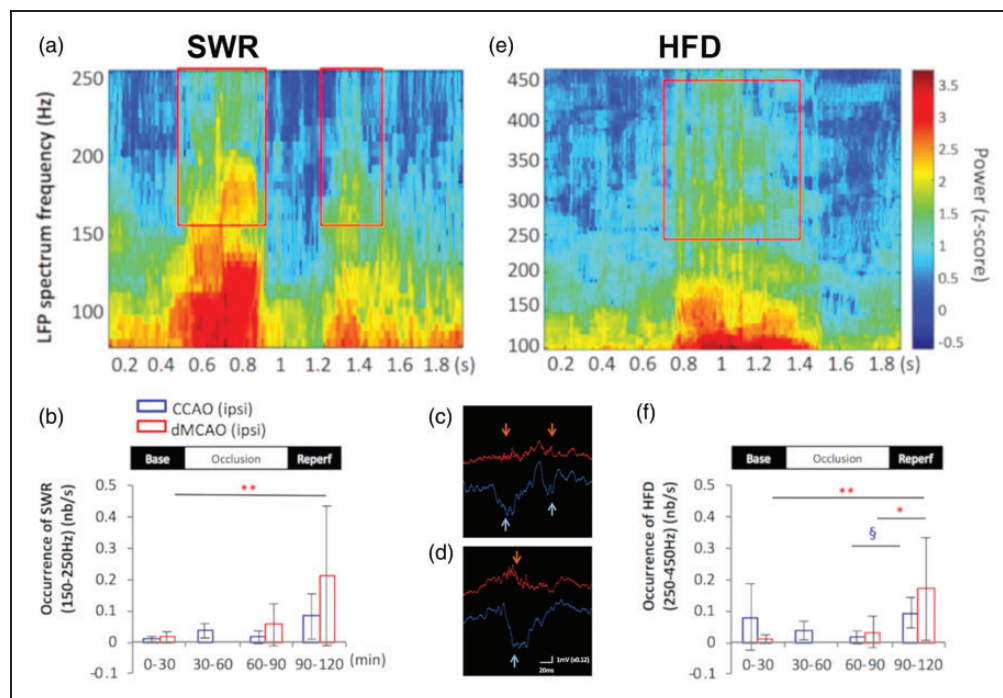


**Figure 4.** Cortical ischemic stroke increased sharp wave associated ripples (SPW-R) and high-frequency discharges (HFD) in the remote hippocampus. a and e, Frequency spectrograms of the LFP recording from CA1 pyramidal layer during dMCAO display the presence of SPW-R in the frequency range of 150–250 Hz (a) and the high frequency discharges in the range of 250–450 Hz embedded in the ripple discharges (e). An increase in the occurrence of SPW-R (b) and HFDs (f) was detected in the ipsilesional CA1 pyramidal layers during MCA reperfusion compared to baseline in the bar graphs. Representative traces show each sharp wave event in the radiatum (light blue arrows) is accompanied by SPW-R (orange arrows) in the CA1 pyramidal layer before stroke (c) and after ischemic-reperfusion with a longer duration of SPW-R (d). Modified from He J et al., figure 2.<sup>48</sup>

continued to shift towards lower frequency oscillation (<1.5 Hz) during reperfusion. Increased  $MI_{HiG}$  in  $\theta$  and low frequencies phases were also detected in the ipsilateral stratum lacunosum-moleculare layer during the dMCAO occlusion period.

The unexpected increase of coupling between cortical  $\gamma$  power and hippocampal  $\theta$  as well as low frequency oscillations during dMCAO occlusion and after reperfusion may reflect an attempt to compensate for the loss of connectivity between the cortex and hippocampus during acute ischemic stroke. The loss of communication between brain regions and the associated increase in phase-amplitude modulation of cortical low  $\gamma$  was previously reported in the near death state of Wistar rats, though with  $\alpha$ - (10–15 Hz) and  $\theta$  oscillations (5–10 Hz).<sup>146</sup> Whether the increased  $\theta$ - $\gamma$  coupling during acute stroke is an effort of the brain to compensate for the temporary loss of cortical input to the hippocampus in the background of large-scale reduction of CBF remains to be verified. In summary, cortical stroke caused an imbalance of excitatory and inhibitory circuits in the remote hippocampus region and disrupted the cortico-hippocampal networks.

*During chronic stroke.* Cognitive impairment is not uncommon among patients after a stroke, even following first-ever stroke.<sup>147</sup> However, how neural activity is chronically affected by cortical stroke in the hippocampal region remote to ischemic infarct is not well characterized. Similar to acute stroke, brain state was disrupted 2–4 weeks after dMCAO as shown by a decreased duration of high  $\theta$  state detected in the bilateral hippocampus, pointing to the persistent nature of altered brain state after ischemic insult.  $\delta$  power appeared to be significantly reduced two weeks after dMCAO compared to non-stroke controls in both the cortex and hippocampus, while  $\gamma$  power peaked at two weeks and gradually reversed back to prestroke level one month after the stroke. Unlike the temporary reduction of hippocampal  $\theta$  and  $\gamma$  power seen during acute stroke,  $\gamma$  power was elevated during chronic stroke possibly due to a compensatory response to the acutely reduced  $\gamma$  oscillatory activity.

Characteristics of SPW-Rs are chronically altered following dMCAO. The signal power of SPW-Rs was increased in the bilateral CA1 pyramidal layer both two weeks and one month after dMCAO. Interestingly, the duration of SPW-R is prolonged two weeks after stroke but is shortened one month after stroke compared to that of the non-stroke control rats. During SPW-R firing, current through the CA1 field of the hippocampus as measured by current source density analysis, revealed pairs of dipoles with the apparent source centered in the pyramidal layer and the sink in the radiatum. Following dMCAO, the

strength of the current dipole increases above baseline at two weeks and then decreases below at one month<sup>49</sup> (Figure 5). Thus, it appears there is a compensatory hyperactivity as a result of stroke that peaks at two weeks after stroke, followed by frequency-specific normalization or restoration to pre stroke level around one month post stroke.

Phase Amplitude Coupling (PAC) between cortex and hippocampus and within the hippocampus is present during high  $\theta$  state where  $\theta$ - $\gamma$  coupling, and  $\delta$ -high  $\gamma$  coupling is present bi-directionally.  $\theta$ - $\gamma$  coupling between the hippocampus and cortex, as well as within the pyramidal layer was significantly lower at IMS compared to non-stroke control (Figure 6). During the low  $\theta$  state, only  $\delta$ -high  $\gamma$  coupling was present which did not change during chronic stroke. The diminished PAC between hippocampal  $\theta$  and cortical  $\gamma$  one month after stroke suggests a persistent breakdown of network communication resulting from ischemic injury, likely caused by the deafferentation of the hippocampal regions from cortical stroke.

### **Effect of environmental enrichment on brain oscillations in chronic stroke and implication in the recovery of function**

Environmental Enrichment (EE) has been widely studied in laboratory animals as an effective method to enhance neuroplasticity, neurogenesis, and to improve behavioral recovery from various brain injury models.<sup>148</sup> With respect to stroke, EE has exerted synergistic effects in enhancing post stroke motor function recovery in rats when combined with task-specific reach training,<sup>149</sup> aside from the many challenges and limitations in translating EE from the bench to clinical practice in rehabilitation medicine. Despite the early skepticism on the efficacy of EE, arguing that the human environment is already enriched compared to the impoverished laboratory animal's environment, increasing evidence has revealed that most stroke patients were in isolation and physically inactive in the hospital setting;<sup>150</sup> this suggests a need to further stimulate and enrich the experience of post stroke patients. Recent evidence suggests that embedding an enriched environment in an acute stroke unit could increase activity in stroke patients.<sup>151</sup> Nevertheless, some foreseeable difficulties have impeded the implementation of EE in clinical practice such as the lack of standard EE paradigms that are essential while conducting clinical trials, or the lack of knowledge in the extent and duration of enrichment to achieve maximal functional recovery, that may vary on an individual level.

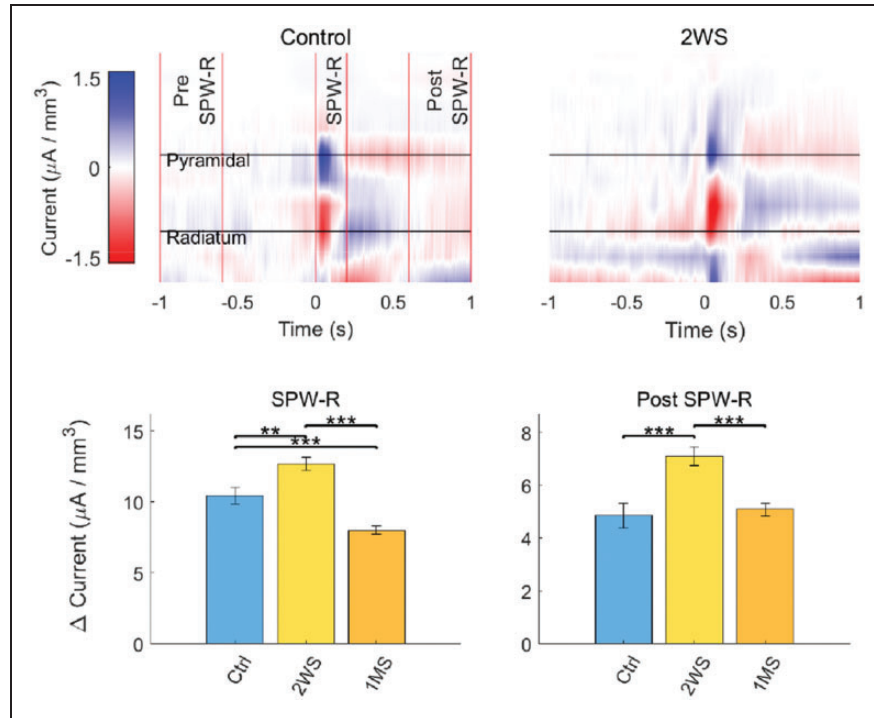


**Figure 5.** Cortical stroke changed the current flow in the hippocampal CA1 layer. Current source density map of ipsilesional CA1 in relation to the timing of ripple firing: before (Pre SPW-R), during, (SPW-R) and after SPW-R (Post SPW-R). Change in local current flow was determined using the difference between the minimum and maximum dipole amplitudes during each time window. An increased current difference was detected at 2 weeks after dMCAO (2WS) and dissipated at 1 month after stroke (1MS). Modified from Ip Z et al., figure 4.<sup>49</sup>

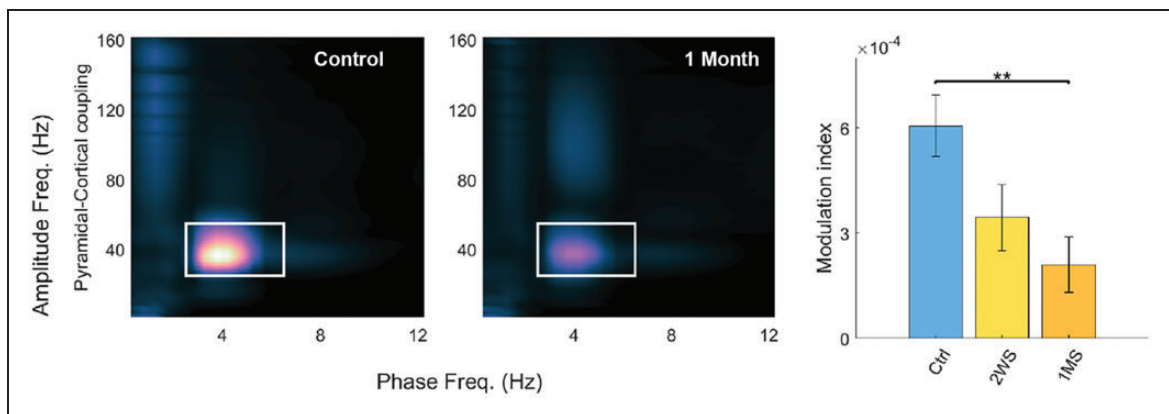


**Figure 6.** Cortical stroke reduced coupling between CA1  $\theta$  and cortical  $\gamma$  oscillations. Phase amplitude comodulograms showing modulation between cortex and hippocampus for control (Ctrl) and 1 month after dMCAO (1MS), in which  $\theta$ - $\gamma$  coupling was demarcated by white rectangle. Significant reduction of average  $\theta$ - $\gamma$  modulation index was detected in rats 1 month after stroke compared to the control rats. \*\*:  $p < 0.01$ . Modified from Ip Z et al., figure 5.<sup>49</sup>

EE has consistently been shown to improve the recovery of motor and spatial memory function following dMCAO stroke (Figure 7). Stroke-induced hypoactivation of limbic regions following maze learning can be visualized via Fos imaging, a proxy of neuronal activation. Housing in the EE for one month after stroke reversed the hypoactivation (Figure 8). As

a physiological correlate of neural function, we wanted to determine whether EE also improved the perturbation of brain oscillations caused by ischemic stroke. EE by itself reduced the signal power of  $\gamma$  in the hippocampus and restored chronic stroke-induced increases of  $\gamma$  power, although it had no effect on  $\delta$  nor  $\theta$  among stroke and non-stroke animals. Exposure to



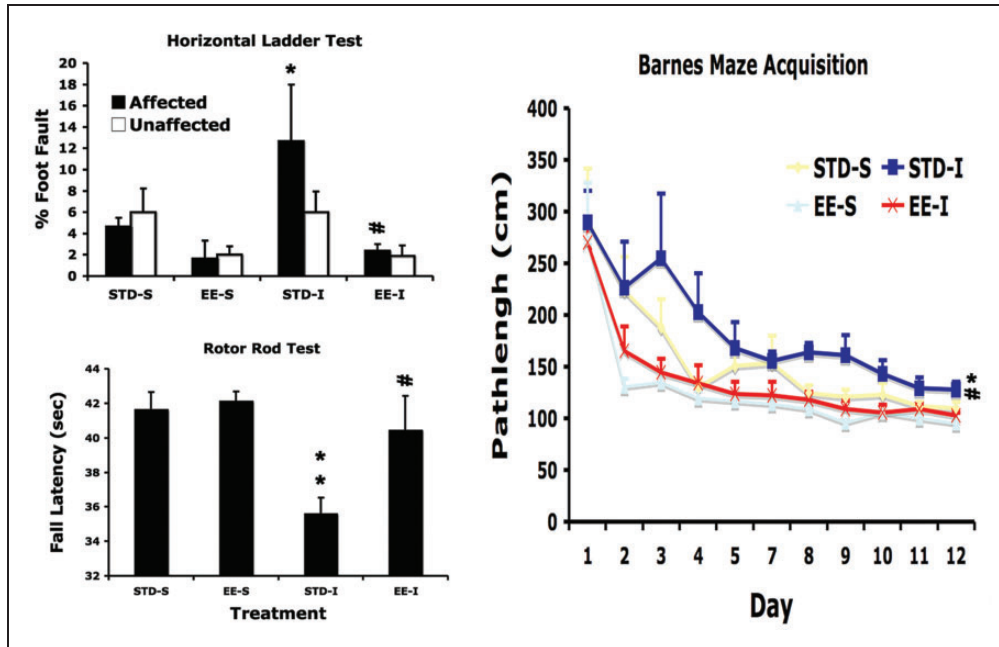


**Figure 7.** Environmental enrichment reduced cortical stroke induced functional impairment. Rats were subjected to either ischemic (I) or sham (S) surgery and housed in either standard- (STD) or enriched environment (EE) one week after surgery for one month. Two-way ANOVA detected a global effect of stroke on motor function impairment 5 weeks after stroke (Ladder test:  $p < 0.05$ ; Rotor rod:  $p < 0.01$ ), while EE had a beneficial effect on both motor and memory function (Ladder test:  $p < 0.05$ ; Rotor rod test:  $p < 0.005$ ; Barnes maze test:  $p < 0.01$ ). Post hoc test detected significant difference between STD-S and STD-I groups (\*:  $p < 0.05$ ; \*\*:  $p < 0.01$ ), and between STD-I and EE-I groups (#:  $p < 0.05$ ; ##:  $p < 0.01$ ).

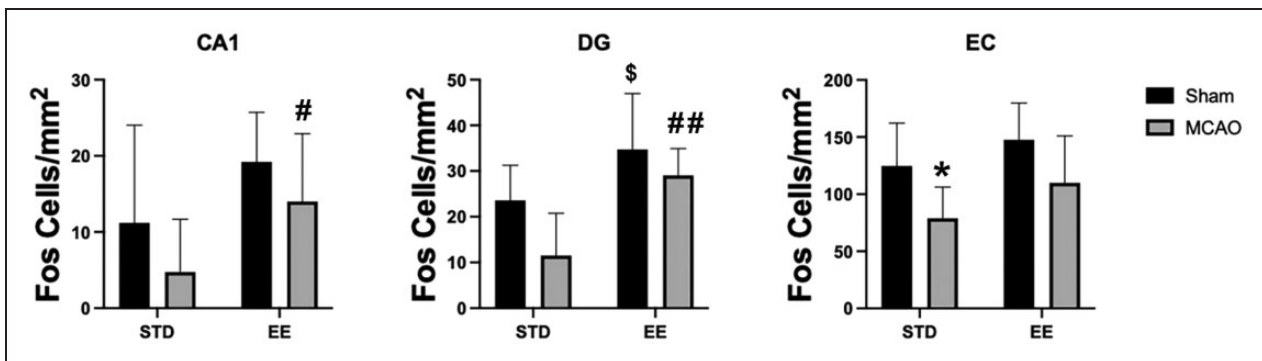


**Figure 8.** Environmental enrichment reversed cortical stroke induced hypoactivation in limbic regions including hippocampal CA1, dentate gyrus (DG) and entorhinal cortex (EC). Ninety minutes after 5-days of training in the Barnes maze, rats were processed for Fos immunohistochemistry. Two-way ANOVA detected a global negative effect of stroke (CA1:  $p < 0.05$ ; DG:  $p < 0.005$ ; EC:  $p < 0.001$ ) and positive effect of enriched environment (EE) (CA1:  $p < 0.005$ ; DG:  $p < 0.001$ ; EC:  $p < 0.01$ ) on Fos immunoreactivity. Specifically, stroke caused hypoactivation in the EC in the STD groups (\* $p < 0.05$ ). EE restored neuronal activation in the CA1 and DG following learning in the Barnes maze relative to standard environment (STD) (Sham EE vs Sham STD: \$ $p < 0.05$ ; MCAO EE vs MCAO STD: ## $p < 0.05$ , ### $p < 0.01$ ).

EE restored HTD in stroke rats, while EE and stroke alone reduced the HTD state. EE mitigated the stroke induced increase to SPW-Rs signal power and decreased its duration, suggesting that EE counterbalanced the excitatory and inhibitory networks disrupted by stroke.<sup>49</sup> Although prolonging SPW-R via optogenetic stimulation of the CA1 neurons reportedly also

improved the memory performance,<sup>54</sup> further studies are needed to understand the optimal SPW-R duration for memory function to differentiate the effects of stroke and EE on the increased duration of SPW-R.

Contrary to its known benefit on synaptic plasticity and cognition, EE unexpectedly lowers the levels of  $\theta$ - $\gamma$  coupling in the hippocampus.<sup>49</sup> Via mechanisms that

are currently unknown, these results suggest there is a reduction of information flow between the cortico-hippocampal networks for both stroke and EE groups. Our results begin to uncover the complex interaction between stroke and EE, albeit further studies in awake animals are warranted to validate these findings and determine the underlying mechanisms. Nonetheless, these neural features may be areas of interest to further understand the network imbalances caused by stroke and to investigate future therapeutic interventions.

### Targeted stimulation-based therapies for stroke

Brain stimulation is believed to modulate the excitability of neural circuits and increase the likelihood of neuroplastic change. Because neurons that fire together, wire together,<sup>152</sup> various approaches combining brain stimulation and rehabilitative training have been proposed to take advantage of stimulation-induced neuroplasticity for neurorehabilitation.<sup>153</sup> In particular it has been shown that repetitive Transcranial Magnetic Stimulation (rTMS), transcranial Direct Current Stimulation (tDCS), and Epidural Cortical Stimulation (ECS) can enhance neural plasticity in the motor cortex post-stroke. The modulatory effects of rTMS have been used in stroke rehabilitation to both induce cortical excitation<sup>154</sup> using high-frequency ( $\geq 3\text{Hz}$ ) rTMS applied to the lesioned motor cortex and induce cortical inhibition<sup>155</sup> using low frequency (near 1 Hz) rTMS to contralesional motor cortex.<sup>156</sup> Similar to rTMS, tDCS has been used for stroke rehabilitation in the motor cortex to both excite lesioned areas using anodal tDCS and inhibit contralesional areas using cathodal tDCS. The rationale behind using these techniques being, that exciting ipsilesional areas promotes rewiring of perilesional neurons to take over lost function and speed the recovery process, while inhibiting the contralesional areas may restore the balance between the two hemispheres.<sup>156</sup> Furthermore, a large body of animal and human studies have shown brain stimulation promotes motor recovery following stroke.<sup>157</sup> This led to the use of ECS in humans which initially looked promising but failed to show significant efficacy in large clinical trials. Although rTMS, tDCS, and ECS all modulate cortical excitability, the induced changes in motor recovery are most effective when combined with motor training.<sup>156</sup> The effects of these stimulation techniques alone on brain physiology and functional recovery remain poorly understood.

More recently, other studies have reported reorganization of the brain using targeted electrical or

optogenetic stimulation,<sup>158–163</sup> that show promise for using these paradigms for neurorehabilitation. In particular, closed-loop activity-dependent stimulation has received more attention due to its dependence of stimulation protocols on the state of the brain.<sup>158–160</sup> In these techniques the stimulation parameters are informed by the activity of the network or a nearby area. Notably, the stimulation protocols are informed by the Hebbian Plasticity model. At the cellular level, connections between two neurons are strengthened when the firing of one neuron repeatedly contributes to the firing of the second, a mechanism termed Hebbian plasticity.<sup>152</sup> Spike Timing Dependent Plasticity (STDP), according to Hebbian rules,<sup>152</sup> states that the probability of connectivity change between two neurons depends on the relative firing time between them. Based on STDP, the probability of any change between two neurons is close to zero if the delay between their firing is more than 100 ms. This probability is highest for small delays such as 5 ms. Activity-dependent stimulation according to STDP rules have been shown to induce more robust neural plasticity,<sup>156,159,160</sup> and restore normal patterns of functional connectivity between cortical regions.<sup>156</sup> It has indicated that activity-dependent brain stimulation in accordance with Hebbian principles<sup>152</sup> may lead to greater recovery from the motor deficits caused by stroke.<sup>156,164</sup> Targeted stimulation in these studies have shown the feasibility of fine-scale changes in functional connectivity both locally<sup>160</sup> and at the network level.<sup>162,163</sup>

Despite the therapeutic promise these techniques have shown, there are major discrepancies that need to be addressed before these techniques can be used for stroke therapy. Previous stimulation techniques haven't been specific enough, and risk unintentionally affecting large areas of the brain and their connections. Technologies with high spatial resolution capabilities are needed to control the off target<sup>163</sup> and widespread network effects.<sup>162</sup> Furthermore, the brain's natural connectivity may play an important role in the plasticity mechanisms and has yet to be incorporated in generating the stimulation protocols. Recent findings show that the underlying network structure is an important mediator of the response to brain stimulation.<sup>165</sup> Moreover, since each injury is unique in various aspects, an optimal stimulation protocol needs to attend to the patient's individualized needs. As stated earlier, strokes may impact both local and distant circuits, which can be reflected in the neurophysiological measures such as coherence and cross-frequency coupling.<sup>166</sup> Recent evidence suggests that brain stimulation has the potential to induce plastic changes and compensate for these functional connectivity alterations following neural damage.<sup>162,166</sup>

Our understanding of the effects of stimulation on brain oscillations and the underlying mechanisms that lead to plasticity change are still in their infancy. Emerging technologies enabling large-scale manipulations of brain circuits such as optogenetics in non-human primates<sup>167–169</sup> can provide significant insight into these underlying mechanisms and galvanize the creation of more sophisticated and personalized stimulation-based therapies for stroke patients.

Apart from direct brain stimulation of the motor cortex, sensory stimulation has been attempted as a treatment of stroke. Although spreading depression<sup>170,171</sup> was reported to be triggered by sensory stimulation following stroke,<sup>132</sup> recent work has contradicted this finding by showing the protective effect of peripheral stimulation within 5 hours of stroke.<sup>172–174</sup> Simultaneous neural recording during sensory stimulation has shown a decrease in the degree of synchrony in LFP that was elevated due to stroke, taking it back to pre-stroke levels. It is possible that the extent of residual blood flow surrounding the stimulation determines the outcome of stimulation. Neural recordings across multiple brain areas during a stroke and following ischemic lesion formation could be critical in understanding the current contradictory results reported on sensory stimulation following stroke.

## Conclusions

The integration of electrophysiological biomarkers obtained from extracellular recordings during acute or chronic stroke will be of great significance to clinical and pre-clinical stroke studies. In the clinical realm, spatial resolution and signal quality continues to improve due to emerging technologies. In both clinical and preclinical stroke research, advances in data mining techniques and sophisticated computer modeling have substantially improved our understanding of the underlying neural mechanisms in response and adaptation to ischemic injury and therapies.

## Funding

The author(s) disclosed receipt of the following financial support for the research, authorship, and/or publication of this article: This work was supported by NIH grant R01NS102886 (JL), R21NS120193 (JL), Research Career Scientist award IK6BX004600 (JL), the Eunice Kennedy Shiver National Institute of Child Health & Human Development of the National Institutes of Health under Award Number K12HD073945 (AY), and the Center for Neurotechnology (CNT, a National Science Foundation Engineering Research Center under Grant EEC-1028725) (AY).

## Acknowledgements

The authors would like to thank Mr. Jaime Falcone-Juengert for manuscript editing.

## Declaration of conflicting interests

The author(s) declared no potential conflicts of interest with respect to the research, authorship, and/or publication of this article.

## Authors' contributions

YS contributes to the section of clinical stroke and recovery  
 OS contributes to the stroke and connectome interpretation  
 ZI contributes to the chronic experimental stroke interpretation  
 GR contributes to the basic LPF/EEG concepts and acute experimental stroke interpretation  
 SO contributes to the clinical stroke knowledge  
 TT contributes to the clinical stroke knowledge and overall support  
 AYS contributes to the concept of brain stimulation and BMI  
 JL contributes to the overall concept, writing and interpretation of clinical and preclinical stroke studies including those from her own lab.

## Supplemental material

Supplemental material for this article is available online.

## References

1. Finnigan S and van Putten MJ. EEG in ischaemic stroke: quantitative EEG can uniquely inform (sub-) acute prognoses and clinical management. *Clin Neurophysiol* 2013; 124: 10–19.
2. Leemburg S, Gao B, Cam E, et al. Power spectrum slope is related to motor function after focal cerebral ischemia in the rat. *Sleep* 2018; 41: zsy132.
3. Lu XC, Williams AJ and Tortella FC. Quantitative electroencephalography spectral analysis and topographic mapping in a rat model of Middle cerebral artery occlusion. *Neuropathol Appl Neurobiol* 2001; 27: 481–495.
4. Lewis S. Techniques: meg in motion. *Nat Rev Neurosci* 2018; 19: 254.
5. Ahlfors SP and Mody M. Overview of meg. *Organ Res Methods* 2019; 22: 95–115.
6. Kaiju T, Doi K, Yokota M, et al. High spatiotemporal resolution ecog recording of somatosensory evoked potentials with flexible micro-electrode arrays. *Front Neural Circuits* 2017; 11: 20.
7. Dubey A and Ray S. Cortical electrocorticogram (ecog) is a local signal. *J Neurosci* 2019; 39: 4299–4311.
8. Buzsaki G, Anastassiou CA and Koch C. The origin of extracellular fields and currents – EEG, ECOG, LFP and spikes. *Nat Rev Neurosci* 2012; 13: 407–420.
9. Mammone N, De Salvo S, Ieracitano C, et al. Compressibility of high-density EEG signals in stroke patients. *Sensors (Basel)* 2018; 18: 4107.
10. Rabiller G, He JW, Nishijima Y, et al. Perturbation of brain oscillations after ischemic stroke: a potential

- biomarker for post-stroke function and therapy. *Int J Mol Sci* 2015; 16: 25605–25640.
11. Buzsaki G. Hippocampal sharp wave-ripple: a cognitive biomarker for episodic memory and planning. *Hippocampus* 2015; 25: 1073–1188.
  12. Llinas RR. The intrinsic electrophysiological properties of mammalian neurons: insights into central nervous system function. *Science* 1988; 242: 1654–1664.
  13. Crunelli V and Hughes SW. The slow (<1 Hz) rhythm of non-REM sleep: a dialogue between three cardinal oscillators. *Nat Neurosci* 2010; 13: 9–17.
  14. Buffalo EA, Fries P, Landman R, et al. Laminar differences in gamma and alpha coherence in the ventral stream. *Proc Natl Acad Sci U S A* 2011; 108: 11262–11267.
  15. Roopun AK, Middleton SJ, Cunningham MO, et al. A beta2-frequency (20–30 Hz) oscillation in nonsynaptic networks of somatosensory cortex. *Proc Natl Acad Sci U S A* 2006; 103: 15646–15650.
  16. Rawlins JN, Feldon J and Gray JA. Septo-hippocampal connections and the hippocampal theta rhythm. *Exp Brain Res* 1979; 37: 49–63.
  17. Gray CM and McCormick DA. Chattering cells: superficial pyramidal neurons contributing to the generation of synchronous oscillations in the visual cortex. *Science* 1996; 274: 109–113.
  18. Whittington MA, Traub RD and Jefferys JG. Synchronized oscillations in interneuron networks driven by metabotropic glutamate receptor activation. *Nature* 1995; 373: 612–615.
  19. Macdonald KD, Fifkova E, Jones MS, et al. Focal stimulation of the thalamic reticular nucleus induces focal gamma waves in cortex. *J Neurophysiol* 1998; 79: 474–477.
  20. Csicsvari J, Jamieson B, Wise KD, et al. Mechanisms of gamma oscillations in the hippocampus of the behaving rat. *Neuron* 2003; 37: 311–322.
  21. Steriade M. Impact of network activities on neuronal properties in corticothalamic systems. *J Neurophysiol* 2001; 86: 1–39.
  22. Buzsaki G. Theta oscillations in the hippocampus. *Neuron* 2002; 33: 325–340.
  23. Battaglia FP, Benchenane K, Sirota A, et al. The hippocampus: hub of brain network communication for memory. *Trends Cogn Sci* 2011; 15: 310–318.
  24. Ognjanovski N, Maruyama D, Lashner N, et al. Ca1 hippocampal network activity changes during sleep-dependent memory consolidation. *Front Syst Neurosci* 2014; 8: 61.
  25. Mitra A, Snyder AZ, Hacker CD, et al. Human cortical-hippocampal dialogue in wake and slow-wave sleep. *Proc Natl Acad Sci U S A* 2016; 113: E6868–E6876.
  26. McNaughton N, Ruan M and Woodnorth MA. Restoring theta-like rhythmicity in rats restores initial learning in the Morris water maze. *Hippocampus* 2006; 16: 1102–1110.
  27. Buzsaki G and Wang XJ. Mechanisms of gamma oscillations. *Annu Rev Neurosci* 2012; 35: 203–225.
  28. Trimper JB, Galloway CR, Jones AC, et al. Gamma oscillations in rat hippocampal subregions dentate gyrus, ca3, ca1, and subiculum underlie associative memory encoding. *Cell Rep* 2017; 21: 2419–2432.
  29. Bragin A, Jando G, Nadasdy Z, et al. Gamma (40–100 Hz) oscillation in the hippocampus of the behaving rat. *J Neurosci* 1995; 15: 47–60.
  30. Ramadan W, Eschenko O and Sara SJ. Hippocampal sharp wave/ripples during sleep for consolidation of associative memory. *PLoS One* 2009; 4: e6697.
  31. Davidson TJ, Kloosterman F and Wilson MA. Hippocampal replay of extended experience. *Neuron* 2009; 63: 497–507.
  32. Wilson MA and McNaughton BL. Reactivation of hippocampal ensemble memories during sleep. *Science* 1994; 265: 676–679.
  33. Foster DJ and Wilson MA. Reverse replay of behavioural sequences in hippocampal place cells during the awake state. *Nature* 2006; 440: 680–683.
  34. Jadhav SP, Kemere C, German PW, et al. Awake hippocampal sharp-wave ripples support spatial memory. *Science* 2012; 336: 1454–1458.
  35. Girardeau G, Benchenane K, Wiener SI, et al. Selective suppression of hippocampal ripples impairs spatial memory. *Nat Neurosci* 2009; 12: 1222–1223.
  36. Girardeau G, Cei A and Zugaro M. Learning-induced plasticity regulates hippocampal sharp wave-ripple drive. *J Neurosci* 2014; 34: 5176–5183.
  37. Novitskaya Y, Sara SJ, Logothetis NK, et al. Ripple-triggered stimulation of the locus coeruleus during post-learning sleep disrupts ripple/spindle coupling and impairs memory consolidation. *Learn Memory* 2016; 23: 238–248.
  38. Norman Y, Yeagle EM, Khuvis S, et al. Hippocampal sharp-wave ripples linked to visual episodic recollection in humans. *Science* 2019; 365: eaax1030.
  39. Logothetis NK, Eschenko O, Murayama Y, et al. Hippocampal-cortical interaction during periods of subcortical silence. *Nature* 2012; 491: 547–553.
  40. Yang M, Logothetis NK and Eschenko O. Occurrence of hippocampal ripples is associated with activity suppression in the mediodorsal thalamic nucleus. *J Neurosci* 2019; 39: 434–444.
  41. Sanda P, Malerba P, Jiang X, et al. Bidirectional interaction of hippocampal ripples and cortical slow waves leads to coordinated spiking activity during NREM sleep. *Cereb Cortex* 2021; 31: 324–340.
  42. Hauer BE, Pagliardini S and Dickson CT. The reuniens nucleus of the thalamus has an essential role in coordinating slow-wave activity between neocortex and hippocampus. *eNeuro* 2019; 6: ENEURO.0365-19.2019.
  43. Ylinen A, Bragin A, Nadasdy Z, et al. Sharp wave-associated high-frequency oscillation (200 Hz) in the intact hippocampus: network and intracellular mechanisms. *J Neurosci* 1995; 15: 30–46.
  44. Stark E, Roux L, Eichler R, et al. Pyramidal cell-interneuron interactions underlie hippocampal ripple oscillations. *Neuron* 2014; 83: 467–480.
  45. Papatheodoropoulos C and Koniaris E. Alpha5gabaa receptors regulate hippocampal sharp wave-ripple activity in vitro. *Neuropharmacology* 2011; 60: 662–673.

46. Atack JR, Bayley PJ, Seabrook GR, et al. L-655,708 enhances cognition in rats but is not proconvulsant at a dose selective for alpha5-containing gabaa receptors. *Neuropharmacology* 2006; 51: 1023–1029.
47. Racz A, Ponomarenko AA, Fuchs EC, et al. Augmented hippocampal ripple oscillations in mice with reduced fast excitation onto parvalbumin-positive cells. *J Neurosci* 2009; 29: 2563–2568.
48. He J-W, Rabiller G, Nishijima Y, et al. Experimental cortical stroke induces aberrant increase of sharp-wave-associated ripples in the hippocampus and disrupts cortico-hippocampal communication. *J Cereb Blood Flow Metab* 2020; 40: 1778–1796.
49. Ip Z, Rabiller G, He JW, et al. Local field potentials identify features of cortico-hippocampal communication impacted by stroke and environmental enrichment therapy. *J Neural Eng* 2021; 18.
50. Gillespie AK, Jones EA, Lin YH, et al. Apolipoprotein e4 causes age-dependent disruption of slow gamma oscillations during hippocampal sharp-wave ripples. *Neuron* 2016; 90: 740–751.
51. Andrews-Zwilling Y, Bien-Ly N, Xu Q, et al. Apolipoprotein e4 causes age- and tau-dependent impairment of gabaergic interneurons, leading to learning and memory deficits in mice. *J Neurosci* 2010; 30: 13707–13717.
52. Witton J, Staniaszek LE, Bartsch U, et al. Disrupted hippocampal sharp-wave ripple-associated spike dynamics in a transgenic mouse model of dementia. *J Physiol* 2016; 594: 4615–4630.
53. Klausberger T, Magill PJ, Marton LF, et al. Brain-state- and cell-type-specific firing of hippocampal interneurons in vivo. *Nature* 2003; 421: 844–848.
54. Fernández-Ruiz A, Oliva A, Fermino de Oliveira E, et al. Long-duration hippocampal sharp wave ripples improve memory. *Science (New York, N.Y.)* 2019; 364: 1082–1086.
55. Hanslmayr S, Staresina BP and Bowman H. Oscillations and episodic memory: addressing the synchronization/desynchronization conundrum. *Trends Neurosci* 2016; 39: 16–25.
56. Heusser AC, Poeppel D, Ezzyat Y, et al. Episodic sequence memory is supported by a theta-gamma phase code. *Nat Neurosci* 2016; 19: 1374–1380.
57. Sirota A, Montgomery S, Fujisawa S, et al. Entrainment of neocortical neurons and gamma oscillations by the hippocampal theta rhythm. *Neuron* 2008; 60: 683–697.
58. Montgomery SM and Buzsaki G. Gamma oscillations dynamically couple hippocampal ca3 and ca1 regions during memory task performance. *Proc Natl Acad Sci U S A* 2007; 104: 14495–14500.
59. Carr MF, Karlsson MP and Frank LM. Transient slow gamma synchrony underlies hippocampal memory replay. *Neuron* 2012; 75: 700–713.
60. Zhang X, Zhong W, Brankač J, et al. Impaired theta-gamma coupling in app-deficient mice. *Sci Rep* 2016; 6: 21948.
61. Barr MS, Rajji TK, Zomorodi R, et al. Impaired theta-gamma coupling during working memory performance in schizophrenia. *Schizophr Res* 2017; 189: 104–110.
62. Guyot LL, Diaz FG, O'Regan MH, et al. Real-time measurement of glutamate release from the ischemic penumbra of the rat cerebral cortex using a focal Middle cerebral artery occlusion model. *Neurosci Lett* 2001; 299: 37–40.
63. Steriade M, McCormick DA and Sejnowski TJ. Thalamocortical oscillations in the sleeping and aroused brain. *Science* 1993; 262: 679–685.
64. Steriade M, Nunez A and Amzica F. A novel slow (<1 hz) oscillation of neocortical neurons in vivo: depolarizing and hyperpolarizing components. *J Neurosci: Off J Soc Neurosci* 1993; 13: 3252–3265.
65. Cohen BA, Bravo-Fernandez EJ and Sances A Jr. Automated electroencephalographic analysis as a prognostic indicator in stroke. *Med Biol Eng Comput* 1977; 15: 431–437.
66. Macdonell RA, Donnan GA, Bladin PF, et al. The electroencephalogram and acute ischemic stroke. Distinguishing cortical from lacunar infarction. *Arch Neurol* 1988; 45: 520–524.
67. Murri L, Gori S, Massetani R, et al. Evaluation of acute ischemic stroke using quantitative EEG: a comparison with conventional EEG and CT scan. *Neurophysiol Clin* 1998; 28: 249–257.
68. Luu P, Tucker DM, Englander R, et al. Localizing acute stroke-related EEG changes: assessing the effects of spatial undersampling. *J Clin Neurophysiol* 2001; 18: 302–317.
69. Finnigan SP, Rose SE, Walsh M, et al. Correlation of quantitative EEG in acute ischemic stroke with 30-day NIHSS score: comparison with diffusion and perfusion MRI. *Stroke: J Cerebr Circul* 2004; 35: 899–903.
70. Machado C, Cuspineda E, Valdes P, et al. Assessing acute middle cerebral artery ischemic stroke by quantitative electric tomography. *Clin EEG Neurosci* 2004; 35: 116–124.
71. Schneider AL and Jordan KG. Regional attenuation without delta (rawod): a distinctive EEG pattern that can aid in the diagnosis and management of severe acute ischemic stroke. *Am J Electroneurodiagnostic Technol* 2005; 45: 102–117.
72. Sheorajpanday RV, Nagels G, Weeren AJ, et al. Reproducibility and clinical relevance of quantitative EEG parameters in cerebral ischemia: a basic approach. *Clin Neurophysiol: Off J Int Feder Clin Neurophysiol* 2009; 120: 845–855.
73. Finnigan S, Wong A and Read S. Defining abnormal slow EEG activity in acute ischaemic stroke: delta/alpha ratio as an optimal QEEG index. *Clin Neurophysiol: Off J Int Feder Clin Neurophysiol* 2016; 127: 1452–1459.
74. Aminov A, Rogers JM, Johnstone SJ, et al. Acute single channel EEG predictors of cognitive function after stroke. *PloS One* 2017; 12: e0185841.
75. Chen Y, Xu W, Wang L, et al. Transcranial doppler combined with quantitative EEG brain function

- monitoring and outcome prediction in patients with severe acute intracerebral hemorrhage. *Crit Care* 2018; 22: 36.
76. Rogers JM, Bechara J, Middleton S, et al. Acute EEG patterns associated with transient ischemic attack. *Clin EEG Neurosci* 2019; 50: 196–204.
  77. Gottlibe M, Rosen O, Weller B, et al. Stroke identification using a portable EEG device – a pilot study. *Neurophysiol Clin* 2020; 50: 21–25.
  78. Finnigan S and Wong A. Towards pre-hospital identification of acute ischemic stroke: the value of QEEG from a single frontal channel. *Clin Neurophysiol* 2020; 131: 1726–1727.
  79. Phillips JB, Williams AJ, Adams J, et al. Proteasome inhibitor ps519 reduces infarction and attenuates leukocyte infiltration in a rat model of focal cerebral ischemia. *Stroke* 2000; 31: 1686–1693.
  80. Williams AJ, Dave JR, Phillips JB, et al. Neuroprotective efficacy and therapeutic window of the high-affinity n-methyl-d-aspartate antagonist conantokin-g: in vitro (primary cerebellar neurons) and in vivo (rat model of transient focal brain ischemia) studies. *J Pharmacol Exp Ther* 2000; 294: 378–386.
  81. Frigeni V, Miragoli L, Grotti A, et al. Neurotolerability of contrast agents in rats with brain ischemia induced by transient Middle cerebral artery occlusion: EEG evaluation. *Invest Radiol* 2001; 36: 1–8.
  82. Zhang S, Tong R, Zhang H, et al. A pilot studies in dynamic profile of multi parameters of EEG in a rat model of transient middle cerebral artery occlusion. *Annu Int Conf IEEE Eng Med Biol Soc* 2006; 1: 1181–1184.
  83. Hartings JA, Rolli ML, Lu XC, et al. Delayed secondary phase of peri-infarct depolarizations after focal cerebral ischemia: relation to infarct growth and neuroprotection. *J Neurosci* 2003; 23: 11602–11610.
  84. Hartings JA, Williams AJ and Tortella FC. Occurrence of nonconvulsive seizures, periodic epileptiform discharges, and intermittent rhythmic Delta activity in rat focal ischemia. *Exp Neurol* 2003; 179: 139–149.
  85. Williams AJ, Lu XC, Hartings JA, et al. Neuroprotection assessment by topographic electroencephalographic analysis: effects of a sodium channel blocker to reduce polymorphic delta activity following ischaemic brain injury in rats. *Fundam Clin Pharmacol* 2003; 17: 581–593.
  86. Lammer AB, Beck A, Grummich B, et al. The p2 receptor antagonist PPADS supports recovery from experimental stroke in vivo. *PLoS One* 2011; 6: e19983.
  87. Moyanova SG, Mastroiacovo F, Kortenska LV, et al. Protective role for type 4 metabotropic glutamate receptors against ischemic brain damage. *J Cereb Blood Flow Metab* 2011; 31: 1107–1118.
  88. Karhunen H, Pitkanen A, Virtanen T, et al. Long-term functional consequences of transient occlusion of the middle cerebral artery in rats: a 1-year follow-up of the development of epileptogenesis and memory impairment in relation to sensorimotor deficits. *Epilepsy Res* 2003; 54: 1–10.
  89. Karhunen H, Nissinen J, Sivenius J, et al. A long-term video-EEG and behavioral follow-up after endothelin-1 induced middle cerebral artery occlusion in rats. *Epilepsy Res* 2006; 72: 25–38.
  90. Kelly KM, Jukkola PI, Kharlamov EA, et al. Long-term video-EEG recordings following transient unilateral middle cerebral and common carotid artery occlusion in long-Evans rats. *Exp Neurol* 2006; 201: 495–506.
  91. Moyanova SG, Mitreva RG, Kortenska LV, et al. Age-dependence of sensorimotor and cerebral electroencephalographic asymmetry in rats subjected to unilateral cerebrovascular stroke. *Exp Transl Stroke Med* 2013; 5: 13.
  92. Andraus ME and Alves-Leon SV. Non-epileptiform EEG abnormalities: an overview. *Arq Neuropsiquiatr* 2011; 69: 829–835.
  93. Shreve L, Kaur A, Vo C, et al. Electroencephalography measures are useful for identifying large acute ischemic stroke in the emergency department. *J Stroke Cerebrovasc Dis* 2019; 28: 2280–2286.
  94. Erani F, Zolotova N, Vanderschelden B, et al. Electroencephalography might improve diagnosis of acute stroke and large vessel occlusion. *Stroke: J Cerebr Circul* 2020; 51: 3361–3365.
  95. Alberto P, Elisabetta F, Paola R, et al. The EEG in lacunar strokes. *Stroke: J Cerebr Circul* 1984; 15: 579–580.
  96. Ajcevic M, Furlanis G, Naccarato M, et al. Hyper-acute EEG alterations predict functional and morphological outcomes in thrombolysis-treated ischemic stroke: a wireless EEG study. *Med Biol Eng Comput* 2021; 59: 121–129.
  97. Finnigan SP, Rose SE and Chalk JB. Rapid EEG changes indicate reperfusion after tissue plasminogen activator injection in acute ischaemic stroke. *Clin Neurophysiol* 2006; 117: 2338–2339.
  98. Bandla A, Liao LD, Chan SJ, et al. Simultaneous functional photoacoustic microscopy and electrocorticography reveal the impact of rtpa on dynamic neurovascular functions after cerebral ischemia. *J Cereb Blood Flow Metab* 2018; 38: 980–995.
  99. de Vos CC, van Maarseveen SM, Brouwers PJ, et al. Continuous EEG monitoring during thrombolysis in acute hemispheric stroke patients using the brain symmetry index. *J Clin Neurophysiol* 2008; 25: 77–82.
  100. Andrews RJ. Transhemispheric diaschisis. A review and comment. *Stroke: J Cerebr Circul* 1991; 22: 943–949.
  101. Finger S, Koehler PJ and Jagella C. The Monakow concept of diaschisis: origins and perspectives. *Arch Neurol* 2004; 61: 283–288.
  102. Cuspineda E, Machado C, Aubert E, et al. Predicting outcome in acute stroke: a comparison between QEEG and the Canadian neurological scale. *Clin Electroencephalogr*. 2003; 34: 1–4.
  103. Xin X, Chang J, Gao Y, et al. Correlation between the revised brain symmetry index, an EEG feature index,

- and short-term prognosis in acute ischemic stroke. *J Clin Neurophysiol* 2017; 34: 162–167.
104. Sheorajpanday RV, Nagels G, Weeren AJ, et al. Quantitative EEG in ischemic stroke: correlation with functional status after 6 months. *Clin Neurophysiol: Off J Int Feder Clin Neurophysiol* 2011; 122: 874–883.
  105. van Putten MJ and Tavy DL. Continuous quantitative EEG monitoring in hemispheric stroke patients using the brain symmetry index. *Stroke: J Cerebr Circul* 2004; 35: 2489–2492.
  106. Cillessen JP, van Huffelen AC, Kappelle LJ, et al. Electroencephalography improves the prediction of functional outcome in the acute stage of cerebral ischemia. *Stroke: J Cerebr Circul* 1994; 25: 1968–1972.
  107. Cohen D. Magnetoencephalography: evidence of magnetic fields produced by alpha-rhythm currents. *Science* 1968; 161: 784–786.
  108. Stefan H, Hummel C, Scheler G, et al. Magnetic brain source imaging of focal epileptic activity: a synopsis of 455 cases. *Brain* 2003; 126: 2396–2405.
  109. Hari R and Kujala MV. Brain basis of human social interaction: from concepts to brain imaging. *Physiol Rev* 2009; 89: 453–479.
  110. Schiffbauer H, Ferrari P, Rowley HA, Berger MS, Roberts TP. Functional activity within brain tumors: a magnetic source imaging study. *Neurosurgery*. 2001; 49: 1313–1320; discussion 1320–1311.
  111. Kiehl A, Deschamps T, Chu RK, et al. Identifying dysfunctional cortex: dissociable effects of stroke and aging on resting state dynamics in meg and fmri. *Front Aging Neurosci*. 2016; 8: 40
  112. Tecchio F, Zappasodi F, Tombini M, et al. Brain plasticity in recovery from stroke: an meg assessment. *Neuroimage* 2006; 32: 1326–1334.
  113. Laaksonen K, Helle L, Parkkonen L, et al. Alterations in spontaneous brain oscillations during stroke recovery. *PLoS One* 2013; 8: e61146.
  114. Gallien P, Aghulon C, Durufle A, et al. Magnetoencephalography in stroke: a 1-year follow-up study. *Eur J Neurol* 2003; 10: 373–382.
  115. Roiha K, Kirveskari E, Kaste M, et al. Reorganization of the primary somatosensory cortex during stroke recovery. *Clin Neurophysiol* 2011; 122: 339–345.
  116. Huang M, Davis LE, Aine C, et al. Meg response to median nerve stimulation correlates with recovery of sensory and motor function after stroke. *Clin Neurophysiol* 2004; 115: 820–833.
  117. Di Rienzo F, Guillot A, Mateo S, et al. Neuroplasticity of imagined wrist actions after spinal cord injury: a pilot study. *Exp Brain Res* 2015; 233: 291–302.
  118. Ghai S, Maso FD, Ogourtsova T, et al. Neurophysiological changes induced by music-supported therapy for recovering upper extremity function after stroke: a case series. *Brain Sci* 2021; 11: 666.
  119. Mohr B, MacGregor LJ, Difrancesco S, et al. Hemispheric contributions to language reorganisation: an meg study of neuroplasticity in chronic post stroke aphasia. *Neuropsychologia* 2016; 93: 413–424.
  120. Silvoni S, Ramos-Murguialday A, Cavinato M, et al. Brain-computer interface in stroke: a review of progress. *Clin EEG Neurosci* 2011; 42: 245–252.
  121. Bray S, Shimojo S and O'Doherty JP. Direct instrumental conditioning of neural activity using functional magnetic resonance imaging-derived reward feedback. *J Neurosci* 2007; 27: 7498–7507.
  122. Buch E, Weber C, Cohen LG, et al. Think to move: a neuromagnetic brain-computer interface (bci) system for chronic stroke. *Stroke: J Cerebr Circul* 2008; 39: 910–917.
  123. Mane R, Chouhan T and Guan C. Bci for stroke rehabilitation: motor and beyond. *J Neural Eng* 2020; 17: 041001.
  124. López-Larraz E, Sarasola-Sanz A, Irastorza-Landa N, et al. Brain-machine interfaces for rehabilitation in stroke: a review. *NeuroRehabilitation* 2018; 43: 77–97.
  125. Mrachacz-Kersting N, Jiang N, Stevenson AJT, et al. Efficient neuroplasticity induction in chronic stroke patients by an associative brain-computer interface. *J Neurophysiol* 2016; 115: 1410–1421.
  126. Nierhaus T, Vidaurre C, Sannelli C, et al. Immediate brain plasticity after one hour of brain-computer interface (bci). *J Physiol* 2021; 599: 2435–2451.
  127. Isbell E, Stevens C, Pakulak E, et al. Neuroplasticity of selective attention: research foundations and preliminary evidence for a gene by intervention interaction. *Proc Natl Acad Sci U S A* 2017; 114: 9247–9254.
  128. Jaaskelainen IP and Ahveninen J. Auditory-cortex short-term plasticity induced by selective attention. *Neural Plasticity* 2014; 2014: 1–11.
  129. Wang W, Collinger JL, Perez MA, et al. Neural interface technology for rehabilitation: exploiting and promoting neuroplasticity. *Phys Med Rehabil Clin N Am* 2010; 21: 157–178.
  130. Zhang SJ, Ke Z, Li L, et al. EEG patterns from acute to chronic stroke phases in focal cerebral ischemic rats: correlations with functional recovery. *Physiol Meas* 2013; 34: 423–435.
  131. Hossmann KA. Viability thresholds and the penumbra of focal ischemia. *Ann Neurol* 1994; 36: 557–565.
  132. von Bornstadt D, Houben T, Seidel JL, et al. Supply-demand mismatch transients in susceptible peri-infarct hot zones explain the origins of spreading injury depolarizations. *Neuron* 2015; 85: 1117–1131.
  133. Ayata C and Lauritzen M. Spreading depression, spreading depolarizations, and the cerebral vasculature. *Physiol Rev* 2015; 95: 953–993.
  134. Sheorajpanday RV, Nagels G, Weeren AJ, et al. Additional value of quantitative EEG in acute anterior circulation syndrome of presumed ischemic origin. *Clin Neurophysiol* 2010; 121: 1719–1725.
  135. Rapp PE, Keyser DO, Albano A, et al. Traumatic brain injury detection using electrophysiological methods. *Front Hum Neurosci*. 2015; 9: 11
  136. Hertle DN, Heer M, Santos E, et al. Changes in electrocorticographic beta frequency components precede spreading depolarization in patients with acute brain injury. *Clin Neurophysiol* 2016; 127: 2661–2667.

137. Biswal B, Yetkin FZ, Haughton VM, et al. Functional connectivity in the motor cortex of resting human brain using echo-planar mri. *Magn Reson Med* 1995; 34: 537–541.
138. Raichle ME, MacLeod AM, Snyder AZ, et al. A default mode of brain function. *Proc Natl Acad Sci U S A* 2001; 98: 676–682.
139. Silasi G and Murphy TH. Stroke and the connectome: how connectivity guides therapeutic intervention. *Neuron* 2014; 83: 1354–1368.
140. Baldassarre A, Ramsey LE, Siegel JS, et al. Brain connectivity and neurological disorders after stroke. *Curr Opin Neurol* 2016; 29: 706–713.
141. Guggisberg AG, Koch PJ, Hummel FC, et al. Brain networks and their relevance for stroke rehabilitation. *Clin Neurophysiol* 2019; 130: 1098–1124.
142. Schmitt O and Eipert P. Neuroviisas: approaching multiscale simulation of the rat connectome. *Neuroinformatics* 2012; 10: 243–267.
143. Schmitt O, Badurek S, Liu W, et al. Prediction of regional functional impairment following experimental stroke via connectome analysis. *Sci Rep* 2017; 7: 46316.
144. Miller SM, Sullivan SM, Ireland Z, et al. Neonatal seizures are associated with redistribution and loss of gabaa alpha-subunits in the hypoxic-ischaemic pig. *J Neurochem* 2016; 139: 471–484.
145. Kim JY, Ho H, Kim N, et al. Calcium-sensing receptor (casr) as a novel target for ischemic neuroprotection. *Ann Clin Transl Neurol* 2014; 1: 851–866.
146. Borjigin J, Lee U, Liu T, et al. Surge of neurophysiological coherence and connectivity in the dying brain. *Proc Natl Acad Sci U S A* 2013; 110: 14432–14437.
147. Sun JH, Tan L and Yu JT. Post-stroke cognitive impairment: epidemiology, mechanisms and management. *Ann Transl Med* 2014; 2: 80.
148. Ohlsson AL and Johansson BB. Environment influences functional outcome of cerebral infarction in rats. *Stroke: J Cerebr Circul* 1995; 26: 644–649.
149. Jeffers MS and Corbett D. Synergistic effects of enriched environment and task-specific reach training on poststroke recovery of motor function. *Stroke: J Cerebr Circul* 2018; 49: 1496–1503.
150. Fini NA, Holland AE, Keating J, et al. How physically active are people following stroke? Systematic review and quantitative synthesis. *Phys Ther* 2017; 97: 707–717.
151. Rosbergen IC, Grimley RS, Hayward KS, et al. Embedding an enriched environment in an acute stroke unit increases activity in people with stroke: a controlled before-after pilot study. *Clin Rehabil* 2017; 31: 1516–1528.
152. Hebb DO. *The organization of behavior. A neuropsychological theory*. New York: Wiley, 1949.
153. Ebajemito JK, Furlan L, Nissen C, et al. Application of transcranial direct current stimulation in neurorehabilitation: the modulatory effect of sleep. *Front Neurol* 2016; 7: 54.
154. Pascual-Leone A, Valls-Sole J, Wassermann EM, et al. Responses to rapid-rate transcranial magnetic stimulation of the human motor cortex. *Brain: J Neurol* 1994; 117: 847–858.
155. Chen R, Classen J, Gerloff C, et al. Depression of motor cortex excitability by low-frequency transcranial magnetic stimulation. *Neurology* 1997; 48: 1398–1403.
156. Edwardson MA, Lucas TH, Carey JR, et al. New modalities of brain stimulation for stroke rehabilitation. *Exp Brain Res* 2013; 224: 335–358.
157. Boonzaier J, van Tilborg GAF, Neggers SFW, et al. Noninvasive brain stimulation to enhance functional recovery after stroke: studies in animal models. *Neurorehabil Neural Repair* 2018; 32: 927–940.
158. Nishimura Y, Perlmutter SI, Eaton RW, et al. Spike-timing-dependent plasticity in primate corticospinal connections induced during free behavior. *Neuron* 2013; 80: 1301–1309.
159. Lucas TH and Fetz EE. Myo-cortical crossed feedback reorganizes primate motor cortex output. *J Neurosci* 2013; 33: 5261–5274.
160. Jackson A, Mavoori J and Fetz EE. Long-term motor cortex plasticity induced by an electronic neural implant. *Nature* 2006; 444: 56–60.
161. Miller KJ, Schalk G, Fetz EE, et al. Cortical activity during motor execution, motor imagery, and imagery-based online feedback. *Proc Natl Acad Sci U S A* 2010; 107: 4430–4435.
162. Yazdan-Shahmorad A, Silversmith DB, Kharazia V, et al. Targeted cortical reorganization using optogenetics in non-human primates. *Elife* 2018; 7
163. Seeman SC, Mogen BJ, Fetz EE, et al. Paired stimulation for spike-timing-dependent plasticity in primate sensorimotor cortex. *J Neurosci* 2017; 37: 1935–1949.
164. Bueteifisch C, Heger R, Schicks W, et al. Hebbian-type stimulation during robot-assisted training in patients with stroke. *Neurorehabil Neural Repair* 2011; 25: 645–655.
165. Scangos KW, Makhoul GS, Sugrue LP, et al. State-dependent responses to intracranial brain stimulation in a patient with depression. *Nat Med* 2021; 27: 229–231.
166. Salimpour Y and Anderson WS. Cross-frequency coupling based neuromodulation for treating neurological disorders. *Front Neurosci* 2019; 13: 125
167. Yazdan-Shahmorad A, Tian N, Kharazia V, et al. Widespread optogenetic expression in macaque cortex obtained with mr-guided, convection enhanced delivery (ced) of aav vector to the thalamus. *J Neurosci Methods* 2018; 293: 347–358.
168. Griggs DJ, Khateeb K, Zhou J, et al. Multi-modal artificial dura for simultaneous large-scale optical access and large-scale electrophysiology in non-human primate cortex. *J Neural Eng* 2021; 18.
169. Yazdan-Shahmorad A, Diaz-Botia C, Hanson TL, et al. A large-scale interface for optogenetic stimulation and recording in nonhuman primates. *Neuron* 2016; 89: 927–939.
170. Dohmen C, Sakowitz OW, Fabricius M, et al. Spreading depolarizations occur in human ischemic stroke with high incidence. *Ann Neurol* 2008; 63: 720–728.



171. Nedergaard M and Hansen AJ. Characterization of cortical depolarizations evoked in focal cerebral ischemia. *J Cereb Blood Flow Metab* 1993; 13: 568–574.
172. Liao LD, Liu YH, Lai HY, et al. Rescue of cortical neurovascular functions during the hyperacute phase of ischemia by peripheral sensory stimulation. *Neurobiol Dis* 2015; 75: 53–63.
173. Pan HC, Liao LD, Lo YC, et al. Neurovascular function recovery after focal ischemic stroke by enhancing cerebral collateral circulation via peripheral stimulation-mediated interarterial anastomosis. *Neurophotonics* 2017; 4: 035003.
174. Frostig RD, Lay CC and Davis MF. A rat's whiskers point the way toward a novel stimulus-dependent, protective stroke therapy. *Neuroscientist* 2013; 19: 313–328.